(12) LEVEL II

DNA 4540F

THE HARDENING OF SATELLITE CABLES TO X-RAYS

TRW Defense and Space Systems Group
One Space Park
Redondo Beach, California 90278

28 February 1978

Final Report for Period 18 January 1977—30 November 1977

CONTRACT No. DNA 001-77-C-0084

APPROVED FOR PUBLIC RELEASE;
DISTRIBUTION UNLIMITED.

THIS WORK SPONSORED BY THE DEFENSE NUCLEAR AGENCY
UNDER RDT&E RMSS CODE B323077464 R99QAXEE50307 H2590D.

Prepared for
Director
DEFENSE NUCLEAR AGENCY
Washington, D. C. 20305

Destroy this report when it is no longer needed. Do not return to sender.

PLEASE NOTIFY THE DEFENSE NUCLEAR AGENCY, ATTN: STTI, WASHINGTON, D.C. 20305, IF YOUR ADDRESS IS INCORRECT, IF YOU WISH TO BE DELETED FROM THE DISTRIBUTION LIST, OR IF THE ADDRESSEE IS NO LONGER EMPLOYED BY YOUR ORGANIZATION.

(12) 53

UNCLASSIFIED

SECURITY CLASSIFICATION OF THIS PAGE (When Data Entered)

(18) DNA, SBIE

REPORT DOCUMENTATION PAGE

READ INSTRUCTIONS BEFORE COMPLETING FORM

1. REPORT NUMBER: DNA 4540F
2. GOVT ACCESSION NO.: AD-A089189
3. RECIPIENT'S CATALOG NUMBER:

4. TITLE (and Subtitle): (6) THE HARDENING OF SATELLITE CABLES TO X-RAYS
5. TYPE OF REPORT & PERIOD COVERED: (9) Final Report, 18 Jan [redacted]—30 Nov 77
6. PERFORMING ORG. REPORT NUMBER:

7. AUTHOR(s): (10) David M. Clement, Robert A. Lowell (17) E503
8. CONTRACT OR GRANT NUMBER(s): (15) DNA 001-77-C-0084

9. PERFORMING ORGANIZATION NAME AND ADDRESS:
TRW Defense & Space Systems Group
One Space Park
Redondo Beach, California 90278

10. PROGRAM ELEMENT, PROJECT, TASK AREA & WORK UNIT NUMBERS: (16) Subtask R99QAXE[redacted]

11. CONTROLLING OFFICE NAME AND ADDRESS:
Director
Defense Nuclear Agency
Washington, D.C. 20305

(11)
12. REPORT DATE: 28 Feb[redacted]78
13. NUMBER OF PAGES: 54

14. MONITORING AGENCY NAME & ADDRESS (if different from Controlling Office): (19) 4540F, AD-E300 908

15. SECURITY CLASS (of this report): UNCLASSIFIED

15a. DECLASSIFICATION/DOWNGRADING SCHEDULE:

16. DISTRIBUTION STATEMENT (of this Report)

Approved for public release; distribution unlimited.

17. DISTRIBUTION STATEMENT (of the abstract entered in Block 20, if different from Report)

18. SUPPLEMENTARY NOTES

This work sponsored by the Defense Nuclear Agency under RDT&E RMSS Code B323077464 R99QAXEE50307 H2590D.

19. KEY WORDS (Continue on reverse side if necessary and identify by block number)

Cables
X-Ray
Hardening
SGEMP
Satellites

20. ABSTRACT (Continue on reverse side if necessary and identify by block number)

Several classes of satellite cables are irradiated in SPIRE Corporation's SPI-PULSE 6000 X-Ray facility in order to identify hardening techniques for cables, and to verify computer models of the X-Ray induced response of cables (MCCABE code). The following techniques for hardening cables are shown to be effective: (1) filling the voids between conductors and insulation; (2) employing coaxial cables rather than cable bundles; (3) reducing the atomic numbers of the conductor materials; (4) using

DD FORM 1 JAN 73 1473 EDITION OF 1 NOV 65 IS OBSOLETE

UNCLASSIFIED

SECURITY CLASSIFICATION OF THIS PAGE (When Data Entered)

409637

20. Abstract (Continued)

conductive plastic coatings between conductors and insulation. The following technique for hardening cables was found to be ineffective: matching atomic numbers between conductors and insulation. Model results generally agreed in sign with experiment. The predicted magnitude of response ranged from an order-of-magnitude too low, to essential agreement within experimental error, depending on how well the voids between conductors and insulation were defined.

CONTENTS

FIGURES

TABLES

1.0 INTRODUCTION

We report the results of X-radiation experiments on satellite shielded cables conducted at SPIRE Corporation using the SPI-PULSE 6000 Bremsstrahlung X-ray source. The objectives of these experiments were two-fold: 1) to investigate various hardening techniques which have been proposed to reduce the X-radiation response of cables, and 2) to verify the cable response model as implemented in the MCCABE Code (Multi-Conductor-CABlE.

The basic phenomenology of cable response to X-rays is fairly well understood and has been reported on by several investigators.[1-4] In an earlier report[5] we undertook a parametric study to determine what cable and source parameters governed the response of cables. Our conclusions, based on that parametric study, were that the following parameters were critical in determining the response of cables:

- gap size (i.e., the voids between conductors and insulation)
- shield thickness
- number of inner conductors
- conductor materials

Of lesser importance were dielectric materials, characteristic impedance, overall size, and photon source spectra. These conclusions are valid when the cables are in vacuum, and the incident flux of x-rays is low enough such that limiting effects from accumulated fields, built up by the kinetic charge transfer, is not sufficient to affect the charge transport. The validity of the latter assumption has also been investigated by the authors in some detail,[6] and we believe that for fluences up to a few tenths of cal/cm^2 (and a pulse width of 10ns) that limiting effects are unimportant.

Based on the present understanding of cable response specific proposals to reduce cable response are now examined. The approach is to investigate as many different classes of cables as possible whose parameters vary in a comprehensible way in order to isolate those parameters which would reduce response. With a few exceptions most of the cables tested are off-the-shelf flight-qualified cables, and therefore the hardening techniques recommended in this report are at least feasible. Whether or not they can or should be optimized has not been answered, but from an SGEMP hardening point-of-view the results are encouraging.

The hardening techniques which are investigated here are as follows:

1) Reduce the size of the gaps between conductors and insulation: In practice this is done by either using semi-rigid cables which, because of their solid tubular construction have smaller voids than braided shield cables, or deliberately filling in the gaps in braided cables.

2) Increase the thickness of the cable's RF shield. This procedure leads to more X-ray absorption in the shield, and therefore a reduced response. In practice, one finds that braided shields come in either single or double wrap, and round braid or flat braid.

3) Coat the conductor-dielectric interface with conductive plastic to shunt deposited charge in the dielectric back to the conductors.

4) Match the atomic numbers of conductors and dielectric materials in order to reduce the amount of deposited charge.

A discussion of the test configuration and cables tested follows in Sects. 2.0 and 3.0 respectively. Photomicrographs of most cables tested are given in the Appendix. Results are presented in Sect. 4. These include a comparison of the MCCABE model predictions with experiment. The MCCABE code was originally documented in Reference 3, and has since been updated in References 7 and 8. The main difference between the two versions is that the electron charge transport routines were completely rewritten to handle the case of dielectrics whose emission efficiencies were comparable to that of conductors,[8] and also the case of flashing deposited on conductors is taken into account.[9] Reference 8 also documents the operation of the code.

The conclusions are presented in Sect. 5.0.

2.0 TEST CONFIGURATION

2.1 Selection of Photon Simulator

The SPI-PULSE 6000 X-ray source was selected for the experiments because its spectrum is reasonably low energy, and both fluence and waveform are fairly reproducible. We had a choice of using the 2½" or 12" cathodes, respectively, and chose the latter. This was for two reasons: 1) we had used the 2½" cathode in the past[9] and wanted a different (softer) spectrum to employ on the cable samples in order to make spectral comparisons; 2) the use of the larger cathode meant that straight samples of cable could be tested, rather than coiled ones. The significance is that coiling the cables introduces gaps, which affect the cable response considerably. This might account for the sample-to-sample variation of equilibrium response observed in the earlier experiments with the 2-1/2" cathode. The disadvantage of the larger area is that the illumination is not as uniform.

The SPI-PULSE 6000 12" cathode was operated in two configurations, which we will refer to as spectrum S and H (soft and hard), respectively. The machine operational parameters are summarized in Table 2.1-1.

Table 2.1-1. Operational Parameters of the SPI-PULSE 6000

	SPECTRUM SPI-S	SPECTRUM SPI-H
cathode size	12½"	12½"
diode gap size	1.5 cm	2.5 cm
diode charging voltage	300 kV	300 kV
tantalum converter thickness	0.0035"	0.0035"

In addition the tantalum converter was covered with a tungsten wire mesh which amounted to about 30% coverage of the cathode.

2.2 Test Configuration

The vacuum chamber and supporting structures to hold the cable samples are shown in Figure 2.2-1. The arrangement was designed to hold either four separate cable samples, or a single cable bundle with a maximum of 7 instrumentation lines measuring the cable individual wire responses. A gold calorimeter, which SPIRE Corporation had used earlier for fluence mapping of the SPI-PULSE 6000 was used for making periodic calorimetric measurements, along with two pin diodes which had been previously calibrated by Dr. J. Wilkenfeld at IRT Corporation. The cassette structure which supported the cable samples had sufficient lead shielding to shield the .046" OD semi-rigid instrumentation wires from X-rays on their way back to the vacuum tank feed-through plate. The instrumentation wires

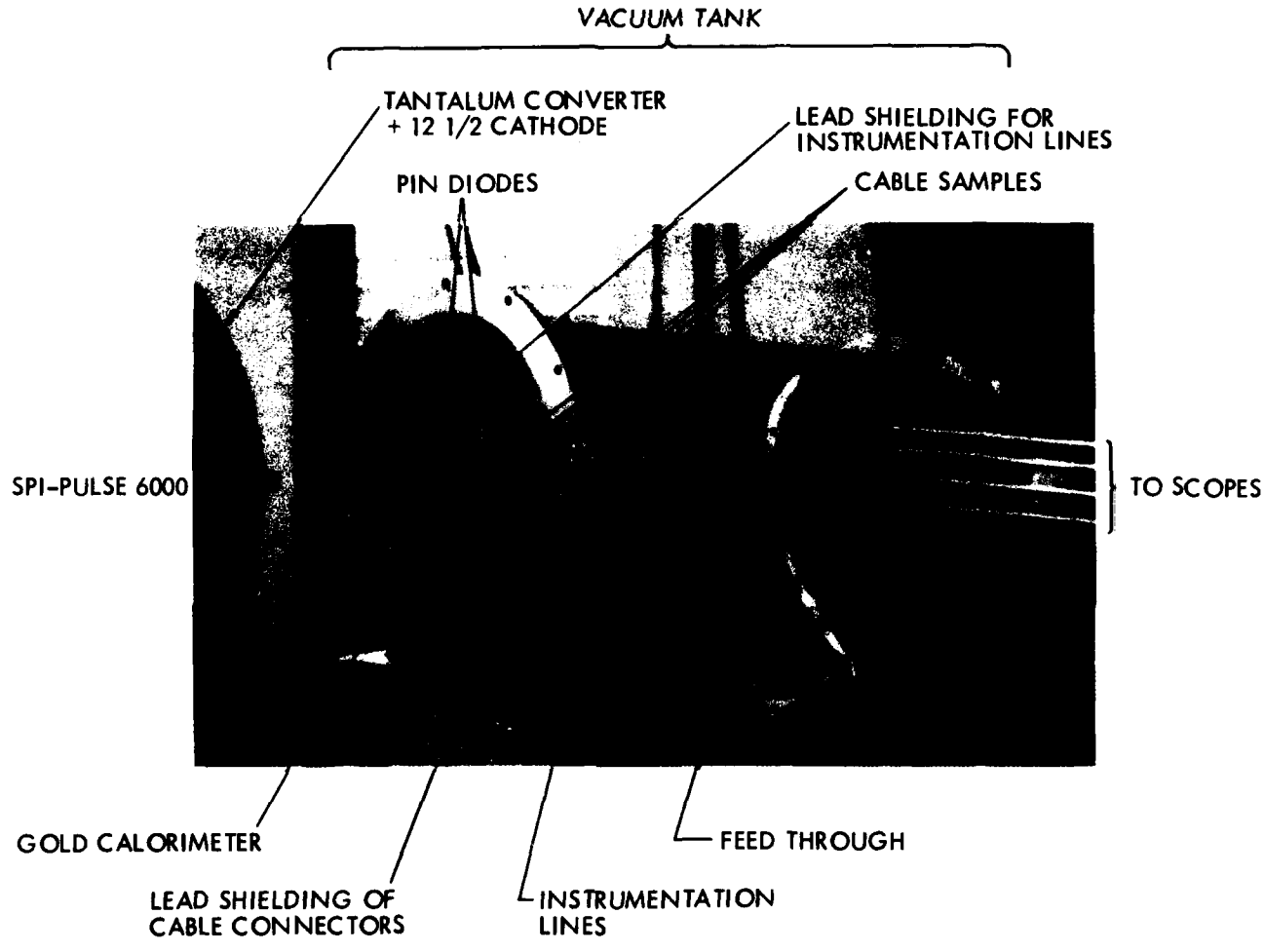

Figure 2.2-1. Cable Test Configuration for the SPI-6000.

were terminated in 50Ω, the nominal scope impedance. Four Tektronix 7844 dual beam oscilloscopes were employed in making the cable response measurements.

The vacuum tank was continuously monitored for air pressure, and the experiments were conducted at pressures of less than 10^{-5} Torr. (A separate experiment involving response as a function of air pressure is reported in Sect. 4.6.) Pump-down time ranged from 30 to 60 minutes except in some cases where, in investigating semi-rigid cables, we pumped down either overnight or over a week-end.

2.3 Source Characteristics of the SPI Pulse-6000

As mentioned in Sect. 2.1 we employed the SPI-PULSE 6000 in two configurations labeled SPI-S and SPI-H. The SPI-S configuration (1½ cm diode gap) has been extensively characterized by one of the authors[10] for the situation where there is no tungsten mesh covering the cathode. The net effect of the mesh is to reduce the fluence and does by 30%, and harden the spectrum slightly. However, a detailed recharacterization of the spectrum, has not been performed and consequently it is assumed that the published spectrum, reproduced in Fig. 2.3-1, is sufficiently accurate to use in the MCCABE model for cable response. For spectrum SPI-H a rough guess is made at the spectrum.

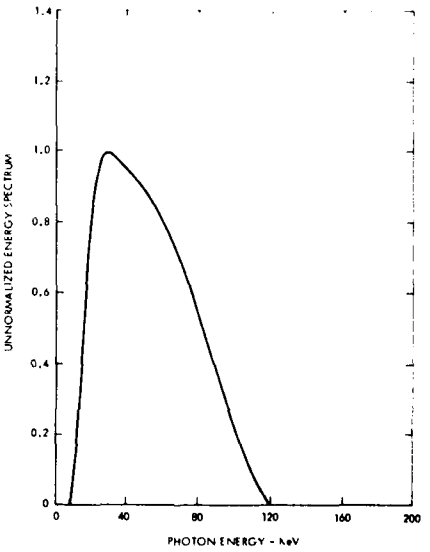

Figure 2.3-1. Spectrum SPI-S for the SPI-PULSE 6000

As mentioned above a calorimeter was used both to measure the fluence at the cable (3 cm from the cathode), pin diodes, and also TLD measurements. With knowledge of the pulse waveform (Figure 2.3-2) one can then extract peak fluxes and dose-rates. These measurements are not independent, however, and in fact three numbers for the total dose for each spectrum can be calculated from the following procedures: 1) that the colorimeter

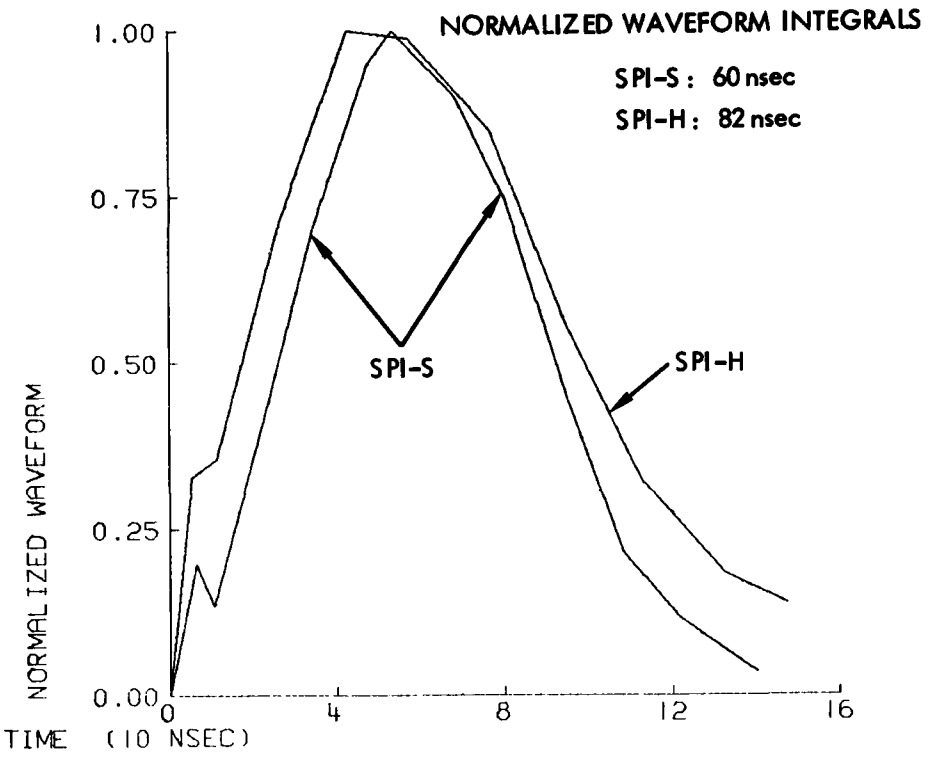

Figure 2.3-2. Cable Response Waveforms for Spectra SPI-S and SPI-H

measurements and the published spectrum and convert to rads(Si) analytically; 2) perform TLD measurements to obtain the rads(Si); 3) take the calibrated pin-diode dose rate in rads(Si)/sec, then integrate the time waveform to obtain the total dose (Figure 2.3-2).

The fluence and dose information is summarized in Table 2.3-1 for each of the three methods mentioned above.

Table 2.3-1. Fluence and Dose at the Cables in the Test Configuration

Spectrum	Fluence ($mcal/cm^2$)	Dose (rads (Si)) (1)[a]	(2)[b]	(3)[c]
SPI-S	0.17 ± 25%	59.5	53 ± 20%	15
SPI-H	0.18 ± 25%		58 ± 20%	12

[a] calorimeter + spectrum

[b] TLD

[c] pin diode + integrated waveform

3.0 CABLE SELECTION AND PREPARATION

A wide variety of satellite cables were selected for the experiments. These are listed in Table 3.0-1, along with their physical dimensions. Cross-sections of most of the cables are presented in a series of photo-micrographs in the Appendix. This detailed information is provided for two reasons: first, the data in Table 3.0-1 represents the input to the MCCABE code which was used to make the test predictions, and secondly, other investigators may wish to verify their own cable models, and the data and photo-micrographs may be useful to them. Also, a summary of insulation properties which was used in the MCCABE calculations is given in Table 3.0-2.

Briefly, the cables tested and the labels for the various classes, used in reporting the results are as follows:

Cable Classes	Labels
Solid semi-rigid	
Al/Teflon/Al	SR-A to SR-D
Al/KelF/Al, Al/Halar/Al	SR-E, SR-F
Al/Teflon/Cu	SR-G
Cu/SiO_2/Cu	SR-H
Cu/Teflon/Cu	SR-I to SR-K
Braided Shield	
coax, double round braid	BR-A
coax, single round braid + solid shield	BR-B
coax, single round braid	BR-C to BR-E
coax, double flat braid	BR-F to BR-J
twisted pairs and triples	BR-J to BR-N
Hollow Semi-rigid	BR-O
Braided Cable Bundles	CB-A to CB-C
Shielded Ribbon Cable	CB-D
Specially Prepared Cable	
Conductive plastic conductor-insulation coating	SP-A to SP-3
Solithane impregnated braided coaxial cable	SP-D

Table 3.0-1(a). Composition and geometry of semi-rigid coaxial cables

Label	Spec No.	Materials Shield/Ins/Wire	Shield Dimensions (cm) t ($\times10^{-2}$)	ID ($\times10^{-1}$)	F ($\times10^{-4}$)	G ($\times10^{-3}$)	Wire Dimensions (cm) ID ($\times10^{-2}$)	OD ($\times10^{-1}$)	F ($\times10^{-4}$)	G ($\times10^{-3}$)
Aluminum conductor semi-rigid coaxial cables										
SR-A[a]	.086" OD 50Ω	AL/TFE/AL	2.4	1.7	0	0	5.1	1.7	0	0.12
SR-B[a]	.100" OD 50Ω	AL/TFE/AL	2.5	2.0	0	0	6.2	2.0	0	0.25
SR-C[a]	.100" OD 100Ω	AL/TFE/AL	2.5	2.0	0	0	1.9	2.0	0	0.12
SR-C*	oil-filled SR-C									
SR-D[a]	.141" OD 50Ω	AL/TFE/AL	2.8	3.0	0	0	9.1	3.0	0	0
SR-E[b]	.141" OD 50Ω	AL/KELF/AL	2.7	2.1	0	0	5.8	2.1	0	0
SR-F[b]	.141" OD 50Ω	AL/HAL/AL	2.8	3.0	0	0	8.0	2.1	0	0
Aluminum shield, copper center wire semi-rigid coax										
SR-G[a]	.141" OD 50Ω	AL/TFE/Cu	2.8	3.0	0	0	9.1	3.0	2.5	0
Copper conductor semi-rigid coaxial cables										
SR-H[c]	.090" OD 50Ω	CK/SIO/CU	3.1	1.7	3.8	0	5.1	1.7	0	0
SR-I[d]	.086" OD 50Ω	CU/TFE/SPC	2.4	1.7	0	0	5.1	1.7	2.5	0
SR-J[d]	.141" OD 50Ω	CU/TFE/SPC	2.8	3.0	0	0	9.1	3.0	2.5	0
SR-K[d]	.046" OD 50Ω	CU/TFE/SPC	1.2	0.9	0	0	3.0	0.9	33.3	0

t = shield thickness
ID = inner diameter
OD = outer diameter
F = flashing thickness
G = gap

AL = aluminum
CK = coppered Kovar
CU = copper
SPC = silvered copper

TFE = teflon
KeLF = KelF
HAL = Halar = Durasan
SIO = 95% SiO_2+ 5% MgO

a) Uniform Tubes
b) Time Wire and Cable
c) Kaman Sciences
d) Precision Tube

Table 3.0-1(b): Composition and geometry of braided and hollow semi-rigid cables

Label	Spec No	Materials Shield/Ins/Wire	Shield Dimensions (cm) t ($\times10^{-2}$)	ID ($\times10^{-1}$)	F ($\times10^{-4}$)	G ($\times10^{-3}$)	Wire Dimensions (cm) ID ($\times10^{-3}$)	OD ($\times10^{-2}$)	F ($\times10^{-4}$)	G ($\times10^{-3}$)
Coax, double round braid										
BR-A	RG400/U (3A009-002)	SC/TFE/SC	4.8	2.8	0.8	2.5	5.2	2.8	2.5	0
Coax, single round braid + solid shield										
BR-B	GORE-TEX	SC/TFEX/SC	3.5	3.6	1.3	0	14.0	3.6	1.5	0
Coax, single round braid										
BR-C	RG316/U (3A009-001)	SC/TFE/SC	1.5	1.5	0.8	4.3	3.4	1.5	2.0	0
BR-D[a)]	PT3-59-50-3 (3A021-002)	TC/PLF/SCA	1.8	1.5	1.0	2.9	2.2	1.5	2.0	0
BR-E	RG180B/U (3A009-003)	SC/TFE/SC	1.7	2.5	1.3	4.2	2.5	2.5	1.8	1.7
Coax, single flat braid										
BR-F[a)]	PT3-33E-26 (3A019-060)	TC/KY/SCA	0.8	0.8	0.8	1.6	4.1	0.8	1.3	0
BR-G[a)]	PT3-59-50-1	TC/PLF/TCB	0.6	1.1	0.8	2.3	4.2	1.1	2.0	0
BR-H[a)]	PT3-33N-22 (3A019-050)	TC/KY/SC	0.7	0.7	1.0	1.4	3.6	0.7	1.0	0
BR-I[a)]	3A002-006	SC/KAP/SC	0.6	1.0	1.3	2.5	7.7	1.0	2.0	0
Coax, double flat braid										
BR-J[a)]	PT3-59-93 (3A021-003)	TC/PLF/SCA	1.7	2.3	1.0	2.5	4.7	2.3	2.5	0
Multi-wire double round braid										
BR-K[a)]	PT3-53RR-18, (3A017-240), 3 wire	TC/PLF/SC	3.6		0.5	NA	11.6	16.4	1.0	0
BR-L[a)]	PT3-53PP-20 (3A017), 2 wire	TC/PLF/SC	2.8	2.8	0.8	NA	9.2	14.0	1.5	0
Multi-wire single flat braid										
BR-M[a)]	PT3-33R-20 (3A019-107), 3 wire	TC/PLF/SC	1.0	3.4	1.0	NA	9.6	14.1	1.5	0

Table 3.0-1(b). Composition and geometry of braided and hollow semi-rigid cables (Continued)

Label	Spec No.	Materials Shield/Ins/Wire	Shield Dimensions (cm) t ($\times 10^{-2}$)	ID ($\times 10^{-1}$)	F ($\times 10^{-4}$)	G ($\times 10^{-3}$)	Wire Dimension (cm) ID ($\times 10^{-3}$)	OD ($\times 10^{-2}$)	F ($\times 10^{-4}$)	G ($\times 10^{-3}$)
BR-N[a]	PT3-33F-26 (3A019-086) 2 wire	TC/PLF/SCA	0.6	1.8	1.0	NA	4.4	8.9	1.3	0
Hollow semi-rigid coax (spline)										
BR-O[c]	3A024-005	AL/TFE/SAL	6.6	10.0	0	282	17.3	2.1	7.6	0

t = shield thickness
ID = inner diameter
OD = outer diameter
F = flashing thickness
G = gap

SC = silvered copper
SCA = silvered copper alloy
TCB = tinned cadmium bronze
AL = aluminum
SAL = silvered aluminum

TFE = teflon
TFEX = expanded teflon
KY = irradiated kynar + polyalkene
PLF = irradiated foamed polyolefin
KAP = kapton

a) Raychem
b) Labarge
c) Precision Tubes

Table 3.0-1(c). Composition and Geometry of Cable Bundles

Label	Spec No.	Materials Shield/Ins/Wire	Shield Dimensions (cm) t ($x10^{-2}$)	ID ($x10^{-1}$)	F ($x10^{-4}$)	G ($x10^{-3}$)	Wire Dimensions (cm) ID ($x10^{-2}$)	OD ($x10^{-2}$)	F ($x10^{-4}$)	G ($x10^{-3}$)
CB-A[a)]	7-wire with liner	TC/KY/SC	2.3	4.3	0.8	20	7.3	9.0	1.5	0
CB-B[a)]	7-wire without liner	TC/KY/SC	2.3	3.6	0.8	NA	7.3	9.0	1.5	0
CB-C[a)]	19-wire without liner	SC/KY/SC	2.3	7.7	0.8	20	9.0	11.0	1.5	0
CB-D[b)]	Ribbon									

t = shield thickness
ID = inner diameter
OD = outer diameter
F = flashing thickness
G = gap
TC = tinned-copper

a) custom made
b) Hughes

Table 3.0-1(d). Composition and Geometry of Specially Prepared Cables

Label	Spec No.	Materials Shield/Ins/Wire	Shield Dimensions (cm) t ($\times 10^{-2}$)	ID ($\times 10^{-1}$)	F ($\times 10^{-4}$)	G ($\times 10^{-3}$)	Wire Dimensions (cm) ID ($\times 10^{-2}$)	OD ($\times 10^{-2}$)	F ($\times 10^{-4}$)	G ($\times 10^{-3}$)
SP-A[a]	semi-conductor doped Raychem Triax	TC/KY/SC	4.8	2.1	2.0	0	3.2	2.1	2.0	0
SP-B[a]	semi-conductor doped Raychem Coax	TC/KY/SC	1.6	2.1	2.0	0	3.2	2.1	2.0	0
SP-C[a]	semi-conductor doped Raychem, 2 wire	TC/KY/SC	1.6	2.6	1.3	NA	8.3	1.3	2.5	0
SP-D[a]	PT3-33N-22 (34019-050), solithane impregnated Coax	TC/KY/SC	0.7	0.7	1.0	0	3.6	0.7	1.0	0

t = shield thickness
ID = inner diameter
OD = outer diameter
F = flashing thickness
G = gap
TC = tinned copper
SC = silvered copper
KY = irradiated Kynar & polyalkene

a) Raychem

Table 3.0-2. Insulation properties

Insulation	Chemical Formula	Density (g/om^3)	Dielectric Constant
Teflon	C_2F_4	2.19	2.1
Kapton	$C_{22}H_5O_{10}N_2$	1.43	2.42
Halar (Durasan)	$C_4H_4F_3Cl$	1.68	2.03
Kel-f	C_2F_3Cl	1.68	2.37
Polyolefin (Polyethylene)	CH_2	0.90	2.3
Kynar (PVF)[b]	C_2H_2F	1.75	2.85
SiO_2[a]	SiO_2	2.2 (0.7)[a]	3.8 (1.6)[a]

a) powdered 95% SiO_2 - 5% MgO in Kaman cable SR-H has an effective density and dielectric constant shown in parentheses.

b) irradrated Kynar and polyalkene is the actual insulation used in the Raychem cables.

All of the cables, including the conductive plastic doped cables, were off-the-shelf varieties. The exceptions were the cable bundles, which were made up from standard hook-up wire and shield braid in a combed lay configuration, and the solithane impregnated cable.

Most of the cable samples had 24 cm of length exposed to the x-rays, and these were straight. The aluminum/aluminum samples obtained from F. Hai and P. Beemer at Aerospace Corporation were around 100 cm long and gently coiled. One end of the cable was left floating, after being capped with copper foil. SMA connectors were used for all but the cable bundles and the hollow semirigid and the connectors were shielded from the x-rays with lead. Standard ITT-Cannon 50-pin connectors were used on the cable bundles.

No particular cable preconditioning procedures (such as biasing or annealing) were employed on the cable samples, with the following exception: the aluminum/aluminum cable samples obtained from Aerospace had previously been irradiated in the Aerospace Dense Plasma Focus machine, (DPF) (Cables SR-A,B,C,D and G).

In this connection it should be mentioned that a fair number of identical cables tested here had been previously irradiated either by ourselves using the SPIRE 2-1/2" chamber or by Aerospace using the DPF. This was done to obtain a spectral comparison of cable response.

4.0 TEST RESULTS

A complete summary of test results for both spectrum SPI-S and SPI-H and pretest predictions for spectrum SPI-S are given in Table 4.0-1. These results represent the total common-mode normalized response of the wires (peak signal current divided by cable length and peak energy flux).

In the subsections below these results are elaborated by discussing the following topics:

- response as a function of cable type (Sect. 4.1)
- special hardening techniques for cables (Sect. 4.2)
- individual wire response of braided cable bundles (Sect. 4.3)
- spectral response of cables (Sect. 4.4)
- comparison of model results with experiment (Sect. 4.5)

4.1 Response as a Function of Cable Type

To get a clearer picture of how cables respond with respect to their various parameters the cables are grouped together roughly according to type in Figure 4.0-1. These results are for spectrum SPI-S and differ from those in Table 4.0-1 in being divided by the total number of wires inside the shield. It seems only fair in comparing classes in cables to compare the average individual wire response rather than the total common-mode response.

Nearly three orders-of-magnitude separate the lowest response cable from the highest in Figure 4.0-1. Note that the cables are grouped together in this figure roughly as a function of cable type. Since cable response depends on several parameters, and not on simply one alone (e.g. shield thickness, gap size, conductor materials), and many parameters are likely to vary in going from one cable to another, this method of presentation should be more instructive.

One can tell a convincing story about the variation as a function of cable type starting with the lowest response cables and making the following comparisons:

Semi-rigid Cables vs. Braided Cables: Semi-rigid cable response is lower than braided cables because they have thicker shields to absorb the x-rays, and to some extent because they have smaller gaps between insulation and shields than do coaxial braided cables. Note that there is some overlap between the semi-rigid cables at the high response end whose conductors are made of copper, and the double-braided coaxial response at the low end, whose conductors are also made of copper.

Table 4.0-1. Total Common Mode Response of Cables $\left(10^{-9} \frac{\text{Coul} \cdot \text{cm}}{\text{cal}}\right)$

Cable	Exp Spectrum SPI-S	Model Spectrum SPI-S	Exp Spectrum SPI-H
Aluminum conductor semi-rigid coaxial cables			
SR-A	+0.012 ±0.006	+0.005	
SR-B	-0.04 ±0.01	-0.001	-0.07 ±0.02
SR-C	+0.007 ±0.003	-0.02	+0.04 ±0.01
SR-C*			-0.14 ±0.07
SR-D	-0.3 ±0.1	-0.02	-0.24 ±0.12
SR-E	-0.18 ±0.06	-0.06	
SR-F	-0.66 ±0.18	-0.1	-0.6 ±0.2
Aluminum shield, copper center wire semi-rigid coax			
SR-G	+0.24 ±0.06	+0.14	-0.7 ±0.2
Copper conductor semi-rigid coaxial cables			
SR-H	-0.12 ±0.03		-0.12 ±0.06
SR-I	-0.30 ±0.30	+0.09	-2.3 ±1.2
SR-J	-0.48 ±0.12	+0.05	-1.9 ±1.2
SR-K	+0.30 ±0.12		
Coax, double round braid			
BR-A	-2.7 ±0.7	-0.7	-2.8 ±0.7
Coax, single round braid			
BR-B	-0.6 ±0.2	-0.5	-1.1 ±0.2
Coax, single round braid			
BR-C	-2.9 ±0.7	-1.6	-3.1 ±0.8
BR-D	-4.2 ±1.4	-1.0	-3.5 ±0.8
BR-E	-0.7 ±0.2	-1.1	-0.7 ±0.2
Coax, single flat braid			
BR-F	-5.2 ±1.3	-2.6	-3.7 ±1.2
BR-G	-0.4 ±0.1	-2.7	-1.8 ±0.6
BR-H	-7.2 ±1.8	-3.9	-5.4 ±1.8
BR-I	-10 ±2	-6.6	-6.6 ±3.0

Table 4.0-1. Total Common Mode Response of Cables $\left(10^{-9} \frac{\text{Coul} \cdot \text{cm}}{\text{cal}}\right)$ (Continued)

Cable	Exp Spectrum SPI-S	Model Spectrum SPI-S	Exp Spectrum SPI-H
Coax, double flat braid			
BR-J	+10 ±2	-1.1	+6.6 ±1.8
Multi-wire, double round braid			
BR-K	-32 ±7	-22	-25 ±7
BR-L	-31 ±7	-20	-24 ±7
Multi-wire single flat braid			
BR-M	-37 ±9	-49	-33 ±8
BR-N	-28 ±7	-38	-17 ±4
Hollow semi-rigid			
BR-O	-19 ±2	-38	-16 ±4
Low resistivity treated cables			
SP-A	-0.2/+0.2	-0.12[b]	-0.3/0.2[a]
SP-B	-1.6/+0.7		-1.0/0.6[a]
SP-C	-0.7/+4.4	-28[b]	-0.4/+4.8
Solithane impregnated cable			
SP-D	-1.5 ±0.2	-2.6	-1.6 ±0.2
7 wire with liner[c]			
CB-A	-6 ±2	-3.4	
7 wire without liner[c]			
CB-B	-12.6 ± 4.2	-7.1	
19 wire with liner[c]			
CB-C	-7.2 ± 1.8		
Ribbon cable			
CB-D	-23 ±4		

[a] First peak and second peak, respectively, of bipolar response
[b] No conductivity included in model
[c] Averabe individual wire response

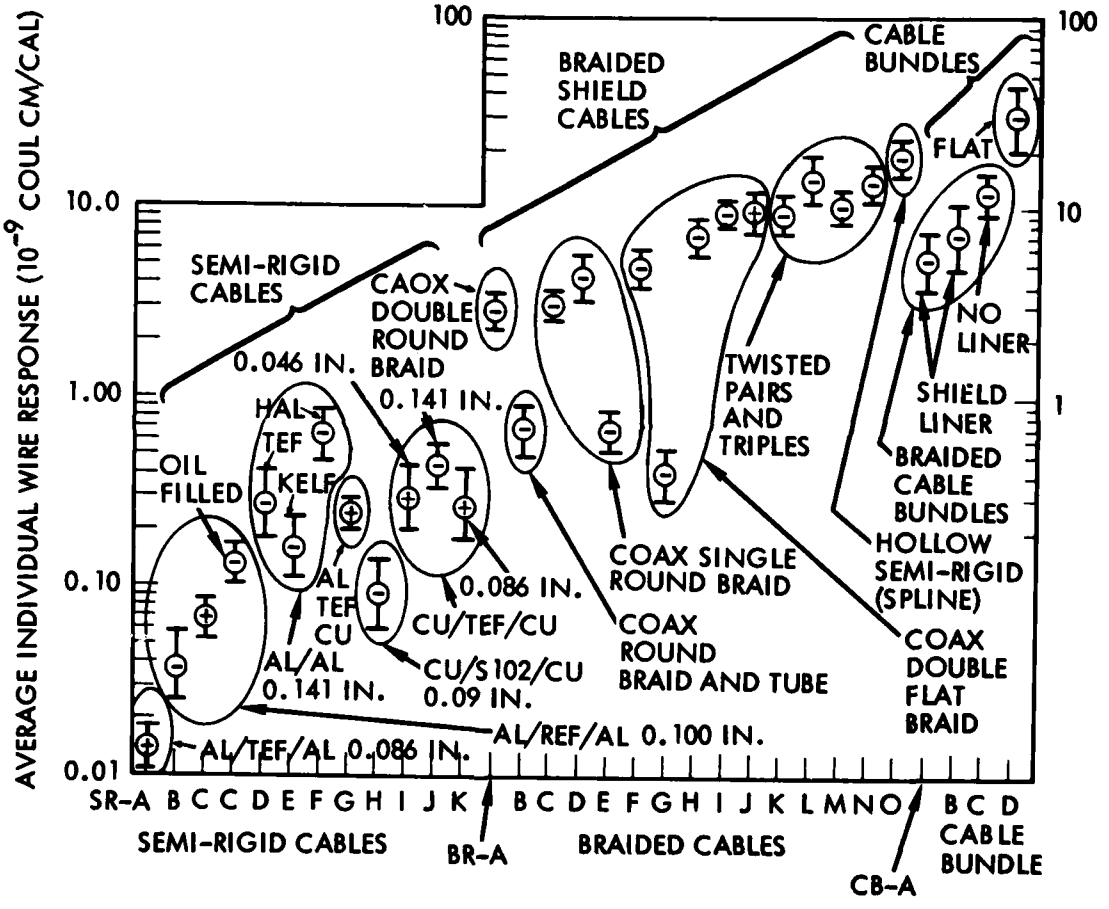

Figure 4.0-1. Average individual wire response for spectrum SPI-S

Aluminum vs Copper Semi-rigid Cables: Reducing the atomic number of the electron emitting materials has a large effect on cable response. The variation of response among the aluminum cables themselves is fairly large, however. In addition to cable size, part of this has to do with uncontrolled gaps at the center wire of aluminum cables which had been reported earlier.[8] Note that when cable SR-C whose response is positive (indicating a center wire gap) was filled with oil (SR-C*), the response changed sign, indicating that electrons from the shield now dominated the response. However, simply changing one of the conductor's emission materials from aluminum to copper is not sufficient to reduce response This is evident in cable SR-G where the shield is aluminum, but the center wire is copper. The response is positive as expected, since the center-wire is made of a higher Z-material, but the response is not lowered compared to the copper-copper cables.

Solid Dielectric Semi-rigid Cable: A possible exception is the copper/SiO_2/copper cable made by Kaman Sciences Corporation (SR-H). It has a slightly thicker shield than the other SR cables and a smaller outer diameter than some. Its low response may be attributed to the use of a powdered silicon-dioxide/magnesium oxide dielectric which is hermetically sealed into the cable and completely fills up the gaps. In contrast, Teflon which tends to flow or creep, will introduce gaps upon bending.

Z-matched Conductor-dielectric Cables: The Halar, KelF and Teflon 0.141" aluminum semi-rigid cables are discussed separately in Section 4.2.2 .

Shield Thickness of Braided Coaxial Cables: Once the decision is made to go to a round braid shield on a coaxial cable, there doesn't appear to be much correlation between the response of single and double round braid, probably because the gap sizes are uncontrollable. Cable BR-B (from Gore) is an exception in that is has a braid outer shield and a semi-rigid (tubular) inner one which apparently reduces the size of the gaps.

However, flat braid cables give a higher response than round braid cables because their shields are less than half as thick (see Table 3.0-1).

Braided Twisted Pairs and Triples: These give a larger response per wire than braided coaxes because there is no insulation to catch the electrons emitted from the shield (see appendix for photo-micrographs of these cables), and a larger fraction of emitted charge will be induced on the center wires than in the coaxial case, even when the amount emitted is the same in both cases.

Hollow Semi-rigid: A (spline) hollow semi-rigid (BR-0) cable which has an enormous gap was tested. The fact that the shield emission material for this cable was aluminum made the cable's response a lot lower than it might have been.

Shielded Bundles: The average individual wire response of these cables was comparable with the twisted pairs and triples. When a shielded liner was added, the response dropped a factor of two. A discussion of the individual wire response separately is given in Section 4.3.

Ribbon Cable: This cable (CB-D) gave a large response presumably because its shields (there are two) were made of silver epoxy.

4.2 Hardening Approaches to Cable X-ray Response

The results of the previous section have emphasized the importance of

- conductor materials
- shield thickness
- gap size

in controlling response of cables. In this section the possibility of deliberately modifying cables to reduce response is discussed. Three possible hardening techniques are discussed:

- filling in the gaps of braided cables (Section 4.2.1)
- matching the atomic numbers of conductor-dielectric materials (Section 4.2.2)
- using conductive plastic coatings at the shield-insulation interface (Section 4.2.3)

4.2.1 Filling the Gaps of Braided Cables

It has already been mentioned that employing a shield liner on a braided cable bundle reduced response by a factor of two. The possibility of drawing up into the cable a molten polymer material such as solithane and allowing it to solidify is considered here. This procedure is attempted on one of our cables (PT3-33N-22, cable BR-H) which is a single flat-braid coax (the modified version is labelled SP-D). Recalling the results from Table 4.0-1 for convenience in Table 4.2.1-1 below:

Table 4.2.1-1. The Effect of Filling the Gaps of a Braided Coax

	Spectrum SPI-S	Spectrum SPI-H
$\frac{\text{impregnated cable response}}{\text{unmodified cable response}}$	0.21	0.29

The effect of the solithane is to produce a 70 to 80% reduction in the cable response.

However, it is rather doubtful that this is a very practical technique for hardening braided cables since the method depends on drawing up the gap-filling material after the braid is applied, not before. But on the other hand that is not to say that some method of laying a closer-wrapped braid on the insulation is not possible.

4.2.2 Conductor - Dielectric Z-Matching

It is not the photo-Compton current density itself that stimulates a cable response, but the divergence of it. In principle, therefore, if one could match the atomic number of a given conductor and the insulation which surrounds it, then the divergence of the current density across an interface would be minimized as well as the rate of charge deposition. In order to investigate this, three aluminum conductor cables which had different dielectrics were tested: Teflon, Halar (Durosan) and Kel-F. The respective chemical formulas for these materials are: CF_2, $C_4H_4F_3Cl$, C_2F_3Cl. It is the presence of chlorine (Z = 17) in Halar and Kel F which provides for a better Z-match with the aluminum conductors.

The normalized response (using spectrum SPI-S) of these three cables are shown in the table below.

Table 4.2.2-1. Response of Aluminum Conductor 0.141" OD Semi-rigid Cables with Z-matched Dielectrics (10^{-9} Coul·cm/cal)

Cable	SPI-S	SPI-H
SR-D Al/Teflon/Al	-0.5	-0.4
SR-E Al/KelF/Al	-0.3	
SR-F Al/Halar/Al	-1.1	-1.0

It can be seen that the Kel-F cable gives a slightly reduced response, but that Halar actually increases the response over Teflon. The response for this behavior may be explained as follows: it is true that the charge deposited in the Halar dielectric is a factor of 2-3 less than in Teflon, but is turns out that the charge penetrates the dielectric more. This is shown in Figure 4.2.2-1 where xf (x) is plotted, where f is fraction of charge which stops in the dielectric a distance x away from the aluminum-dielectric interface. These curves were calculated by the MCCABE Code using the Dellin-MacCallum formalism for the charge profile at the interface.

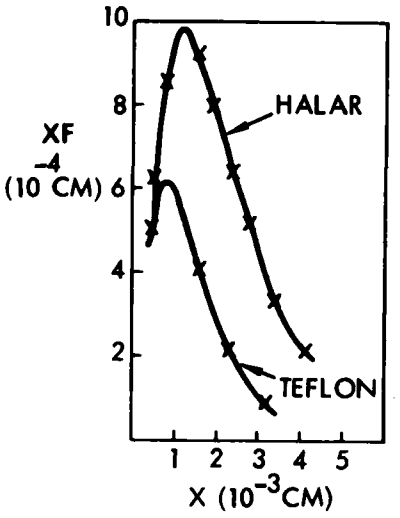

Figure 4.2.2-1. Distribution of deposited charge in dielectric at aluminum/dielectric interface for Teflon and Halar

One concludes that reducing the deposited charge is not sufficient to reduce the response if the reduced charge spreads out more in the dielectric. Recall that the image current response is proportional not only to the total charge deposition rate, but also the distance the electrons travel into the dielectric. It is concluded that at least for this class of dielectrics, Z-matching is not particularly helpful in obtaining low response cables.

4.2.3 Conductive Plastic Coating of Shield-Insulation Interface

Another possible radiation hardening technique for cables is to coat the interfaces between conductors and interfaces with materials of low resistivity. The reasoning is that the charge which is deposited in cables is usually done so near the conductor/insulation interface that a low resistivity coating will shunt the deposited charge back to the conductors before an image current has a chance to get established.

Fortunately it was possible to obtain some braided cables manufactured by Raychem Corporation which had around 4 mils of low resistivity coatings of carbon-loaded polyethylene (conductive plastic) at the shield insulation interface. These cables are used in microphone applications where the effect of the low resistivity material is to reduce static. The value of the resistivity quoted by Raychem officials is on the order of 30 Ω-cm, which would correspond to a time constant $(\varepsilon\rho)^{-1}$ of 10^{-12} sec. Such a small time constant indicates that the shield electron emission may be shunted instantaneously considering the radiation pulse width in our experiments. Three cables were tested.

The first was a triax (SC-A), the second was a coax which was made by stripping the outer shield and its insulation from the triax. (The low resistivity material in this cable was located on the inner side of the inner shield). The third was a twisted shielded pair (TSP). Results using spectrum SPI-S are shown in Figure 4.2.3-1 for the coax and TSP, where for comparison a standard braided coax (RG316/U) and TSP (PT3-33F-26) have been shown. We make the following comments:

- in both cases the treated cable gives a lower response, with the TSP nearly an order of magnitude lower;
- both waveforms of the treated cables have the characteristic conductivity signature, i.e., the cable response tries to follow the pulse, but is soon overcome by the conductivity, and the signal reverses sign. Also, for the treated coax, the response significantly outlasts the radiation pulse.

In the case of the treated TSP the competition is fierce between conductivity and shield emission at the outset of the pulse. The positive portion of this amplitude is interpreted as being stimulated by the center-wire electrons that do not have the benefit of a shunt path as do the electrons deposited near the shield.

The fact that the time constant argument made above does not work as well for the coax is a bit distrubing. Perhaps the electrical contact between the low resistivity material and the shield and its insulation is not as good as expected, and in any case, according to information from Raychem officials, the quoted resistivity for conductive plastic in the bulk is not necessarily the same as when the material is extruded onto a cable.

Results obtained with the triax are qualitatively the same as for the coax, except the amplitude is reduced by half an order-of-magnitude, presumably because of the increased shielding. Finally, all three cables were also shot with spectrum SPI-H (2.5 cm gap) and the responses were 10-20% lower due to the harder spectrum.

4.3 Individual Wire Response of Braided Cable Bundles

Three custom cables were built consisting of either 7 or 19 hook-up wires in a combed lay arrangement, and sheathed with standard braid shield. Two of the cables had a shield inner liner of heat shrinkable tubing, but no special attempt was made to bond the shield to the liner. The objectives were to see how the cable currents distributed themselves in a combed lay arrangement.

Results are shown in Figure 4.3-1. The following observations concerning the figure are made:

1) There is generally a gradual fall-off in the response of the outermost wires as one moves from front to back, with the wires closest to the irradiation experiencing the largest response. This is accounted for by the self-screening of the individual wires to the X-rays.

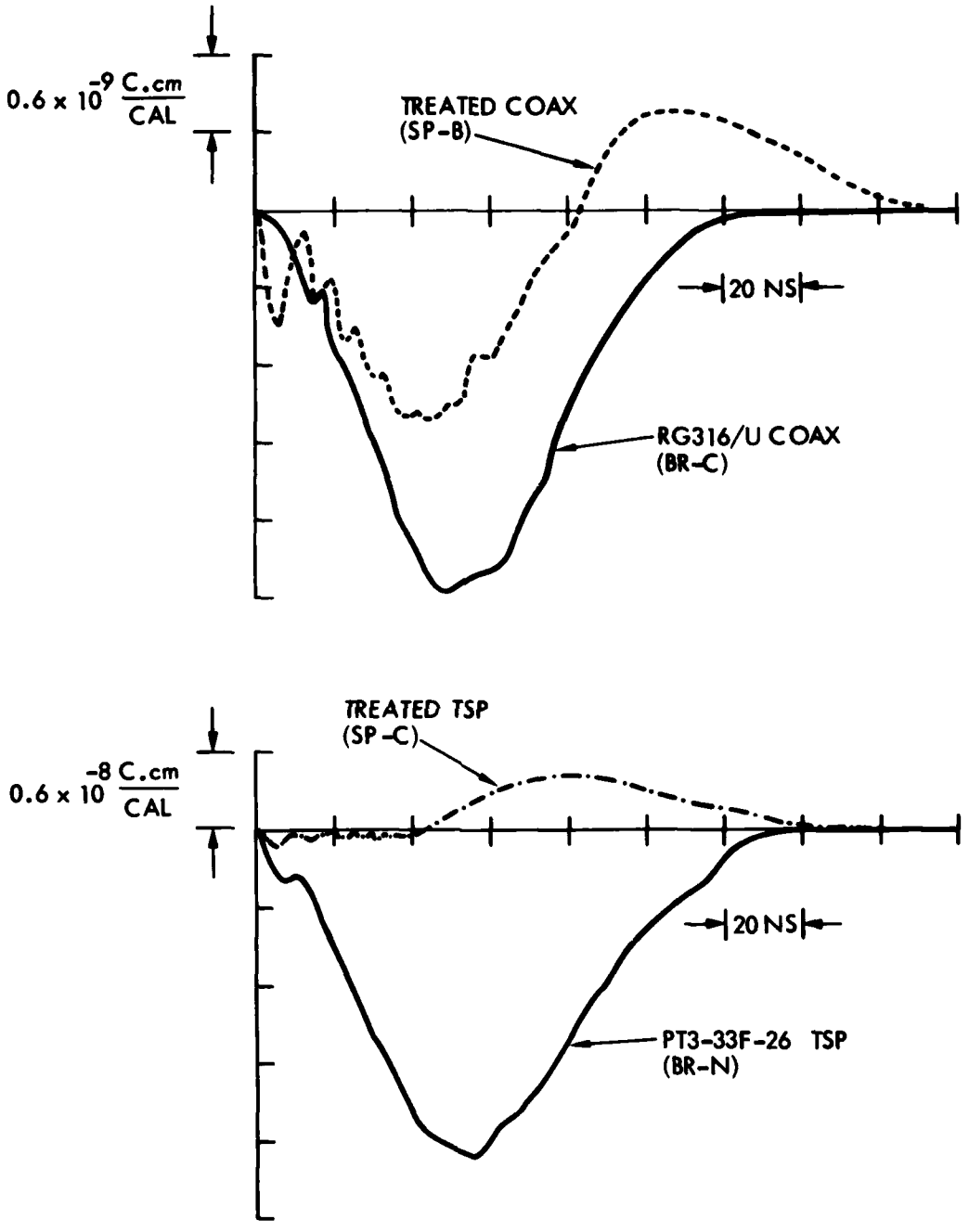

Figure 4.2.3-1. Response of cables treated with conductive plastic

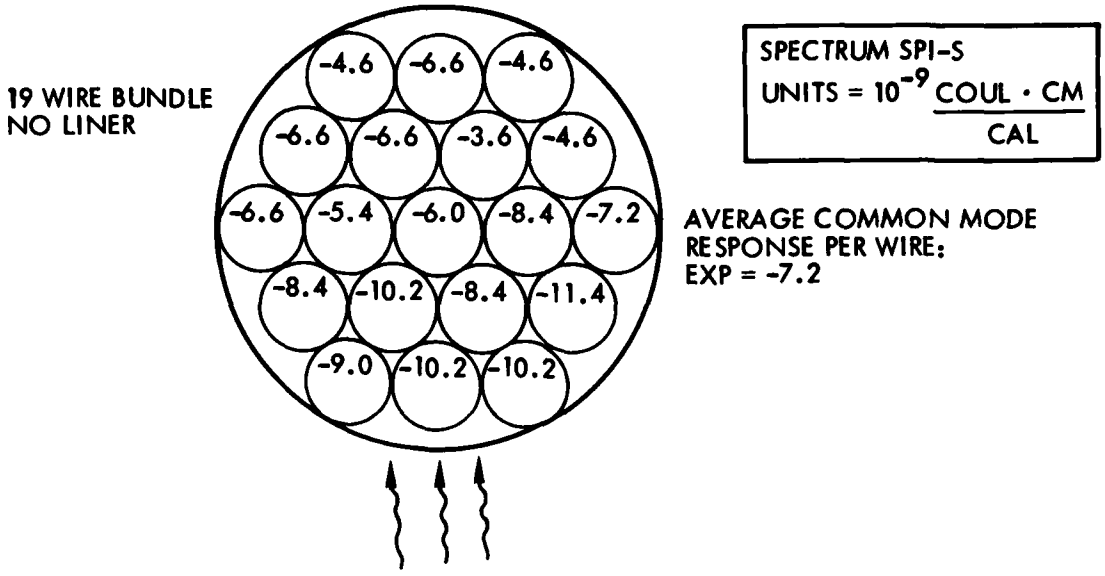

Figure 4.3-1(a). Response of a 19-wire bundle with shield liner

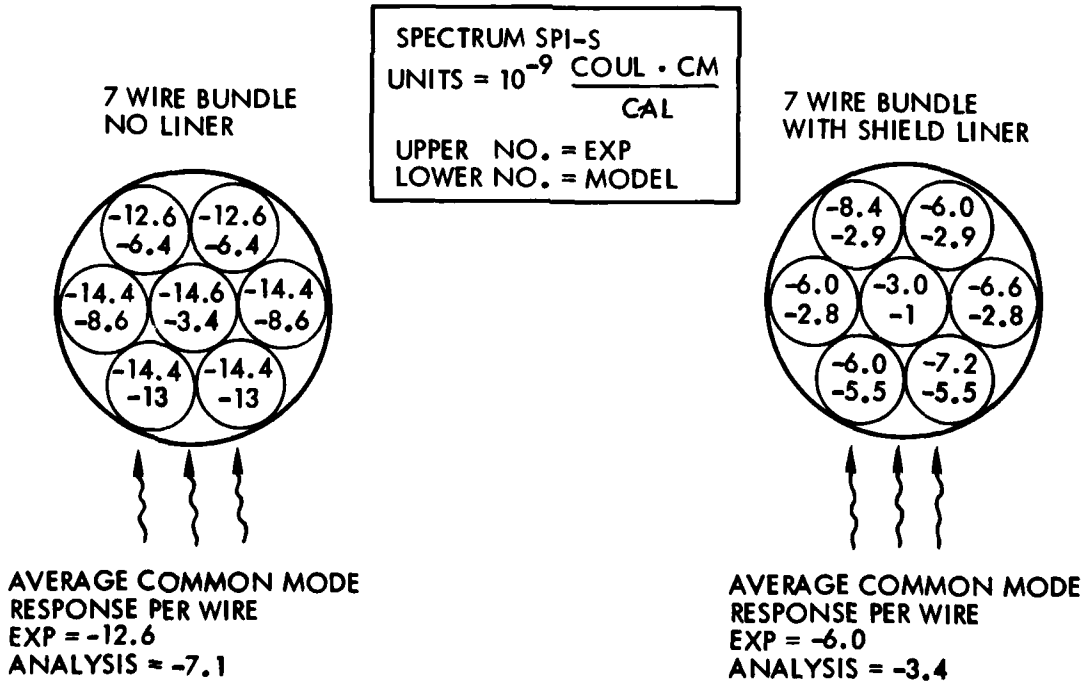

Figure 4.3-1(b). Response of seven wire bundles, with and without shield liner

2) The inner wires, particularly the center wire, has a response which is less than the outer ones. This is interpreted as capacitive screening by the outer wires of the inner ones from the shield.

3) The model indicates that the shield emission of electrons dominates the cable response. This is verified by the fact that the response of all individual wires is negative.

4) The effect of the shield liner is to reduce the response by a factor of two.

One concludes from the results that the variation of individual wire response in a combed lay arrangement is not terribly great (a factor of 2 or 3), at least for this kind of braided shield arrangement. This implies that one could reduce the number of individual wire measurements in large cable bundles: Either one could make representative individual wire measurements leaving unmeasured wires open (or terminated in 50Ω), or else one could combine individual wire measurements with sector current measurements, that is, groups of wires could be joined common mode, before they are measured. The grouping of the wires into sectors is somewhat arbitrary, but pretest modeling of the individual wire response could resolve this.

4.4 Spectral Response of Cables

Next consider the normalized response of cables vs incident spectrum. In order to do so one must compare the response of identical samples, and in addition it is better to compare the responses in normalized units of Coul/rad(Si)·cm rather than Coul·cm/cal since one can show analytically that the former is less sensitive to spectra than the latter. We will return to this point after the comparisons have been made.

In addition to the spectra obtained in this work, results are reported from the following spectra:

- SPI Pulse-6000: 2-1/2" cathode, 200 kV diode charging voltage, obtained from Ref. 9.
- Aerospace Dense Plasma Focus: 6 spectra, obtained from Refs. 2 and 8.

The comparisons are made in Table 4.4-1. The spectra are ordered by the number of rads (Si) that each spectrum yields per cal/cm^2. In other words, reading Table 4.4-1 from left to right, the spectra go from soft to hard.

The following observations are made concerning Table 4.4.1.

1) The results from the various spectra compare favorably, with usually much less than an order of magnitude difference between the lowest and highest spectral response of a given cable.

2) There doesn't appear to be any particular pattern in moving through the spectra from soft to hard. This is probably a good thing from the standpoint of trying to figure out how a cable will respond to an arbitrary spectrum.

Table 4.4-1. Comparison of identical cable responses for different spectra. Besides the spectra reported in this work, the remaining spectra are SPI-2-1/2 from Ref. 9 and various Dense Plasma Focus spectra (DPF) from Refs. 2 and 8.

Cable \ Spectrum rads(Si)/cal	SPI-S_5[a] 1.9×10^5	DPF-O_5 2.4×10^5	SPI-2-1/2 1.3×10^5	DPF-1_4 9.5×10^4	DPF-2_4 6.2×10^4	DPF-B_4 4.8×10^4	DPF-3_4 4.6×10^4	DPF-4_4 3.8×10^4	DPF-5_4 3.4×10^4
	Cable Response $\left(10^{-14}\ \frac{\text{Coul}}{\text{rad(Si)}\cdot\text{cm}}\right)$								
Aluminum/aluminum SR									
SR-A	0.004			0.01					0.01
-B	-0.012	-0.003			0.005		0.12		
-C	0.016	0.007		0.016	0.025		0.031		0.021
-D	-0.102			-0.027					-0.043
-F	-0.222			-0.065	-0.08		-0.045		-0.035
Aluminum/copper SR									
SR-G	0.078			0.18					0.57
Copper/silvered copper									
SA-I	0.102	0.03	1.1		0.08			0.15	
-J	-0.162	-0.02	-1.2		+0.06/ -0.07[a]	<0.1	+0.1/ -0.04[b]	0.08	0.17
Braided coax									
BR-B	-0.24			-0.07			-0.27		-0.25
-H	-2.4		-4.7			-3.7			
-I	-3.6		-18						
-J	-3.6		16			2.5			
Braided pairs and triples									
BR-K	-10.8		-39			-35			
-M	-12.0					-28			
-N	-9.0					-15			
Hollow SR									
BR-O	-6.6					-16			

[a] 35 rads(Si) assumed incident on cable, based on incident fluence and spectrum, Table 2.3-1
[b] sign change observed for 2 distinct samples

If the comparison had been made in normalized units Coul·cm/cal, the situation would be different. This is demonstrated in table below for one of the braided coax cables (BR-H)

Table 4.4-2. Comparison of Normalized Responses for Cable PT3-33N-22 (BR-H) in Coul·cm/cal and Coul/rad(Si)cm

Spectrum	$\left(10^{-9} \frac{\text{Coul·cm}}{\text{cal}}\right)$	$\left(10^{-14} \frac{\text{Coul}}{\text{rad(Si)·cm}}\right)$
SPI-S	-7.2	-2.4
SPI-2-1/2	-6.1	-4.7
DPF-B	-1.8	-3.7

The reason why the one way of reporting is more sensitive to spectra than the other can be seen as follows. Suppose the attenuation of the photons through the cable is ignored and consider a monochromatic beam of photons whose incident flux is 1 cal/cm^2-sec. The response in Coul·cm/cal will be proportional to the electron yield in the conductor, and the incident number flux which is inversely proportioned to photon energy. The yield is proportional both to the absorption cross-section, and the electron range in the conductor which itself is roughly proportional to the energy. The net result is that the Coul·cm/cal result is proportional to the conductor's cross-section, which is strongly energy dependent. However, this is divided by the dose rate which is also proportional to the cross-section of the absorbing material then the explicit energy dependence cancels out, provided one assumes that rads (conductor) and rads (absorbing material) have the same dependence on energy.

4.5 Comparison of Model Results with Experiment

The MCCABE pretest predictions are compared with the experimental common mode results obtained using the SPI-S spectrum. The results are shown in Figure 4.5-1 where the ratio (model response)/(experimental response) is plotted versus cable sample. If the results agree in sign, a plus is indicated; otherwise a minus is shown.

In examining the figure the following observations can be made:

1) The model results tend to be on the low side by at least a factor of 2, but the sign for the most part is correctly predicted

2) There seems to be a pattern in the disagreement between theory and experiment. As one moves in the direction of cables whose gaps are increasingly well defined, for example, the hollow semi-rigid, the agreement gets better

3) Coversely as one moves in the direction of cables whose gaps are less well defined, as in the semi-rigid cables, the agreement gets progressively worse.

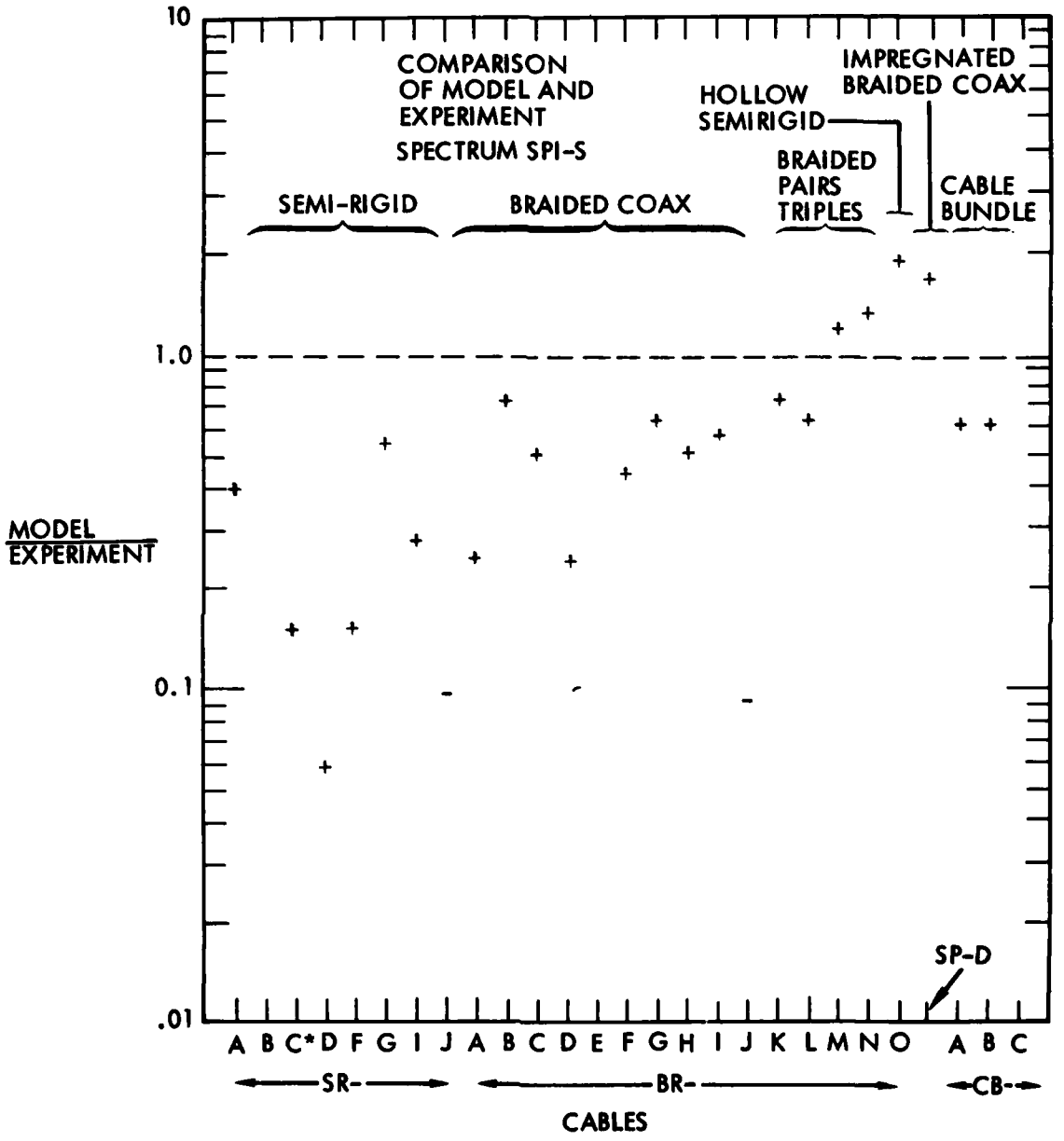

Figure 4.5-1. Comparison of model and experimental cable responses (SPI-S)

Now if it is a question of a factor of two or three disagreement we are not too concerned since there is at least that much uncertainty in the experimental fluence on the other hand and the gap size on the other, either one of which might be adjusted to give better agreement. (The experimental normalized results depend inversely on the measured fluence, while the model results, we have shown in Refs. 3 and 5, are directly proportional to gap size.) The fact that the hollow semi-rigid cable, which is a well-defined geometrical entity with a huge gap that is easily measurable and yields model results within experimental error gives us confidence that the basic physical model and electron transport theory is sound.

What is disturbing however, is the aluminum semi-rigid cable comparisons, most of the model results of which are more than an order-of-magnitude low. Since favorable model comparisons with the Aerospace DPF results had already been made, [8] and are reduced below in Figure 4.5-2, agreement at least as good was expected. In addition the other experimental setup and cable samples themselves were identical with the Aerospace arrangement. Of course, one could always adjust the gap sizes in the model, but it hardly seems fair to use two distinct gaps in the model to predict results of different experiments. On the other hand the response of cables with small or non-existent gaps actually represents the difference of two large numbers, representing shield and center-wire electron emission. If one doubles the size of the gap (say, from 1μ to 2μ) one can produce more than an order-of-magnitude variation in the final result, or even change its sign. It was seen in one experiment (cable SR-C and -C*) that filling up the 2.5μ center-wire gap with oil not only doubled the response but also changed the sign.

Finally, we comment on the sign predictions. The model generally gets this right. One exception worthy of comment is cable BR-J, which is a braided coax with a foamed dielectric. Experimentally the sign is positive presumably indicating gaps at the center wire. This cable was tested in an earlier set of experiments and the same results were found. (Ref. 9, cable PT3-59-93.) However, when the cable was annealed the response became negative, indicating that the foamed dielectric is somehow collapsing onto the center wire, thus filling the gap.

4.6 Response of Cables in Air

Of some interest is the value of the air pressure inside the cable where the "vacuum" response begins to look like a response in air. A typical vacuum response, such as that shown in Figure 2.3-2, follows the radiation pulse, whereas the response in air tends to be bipolar, indicating the competition between emission currents and air shunt currents. To examine this question some cable samples were shot by varying the tank air pressure from shot-to-shot. It should be pointed out that the air

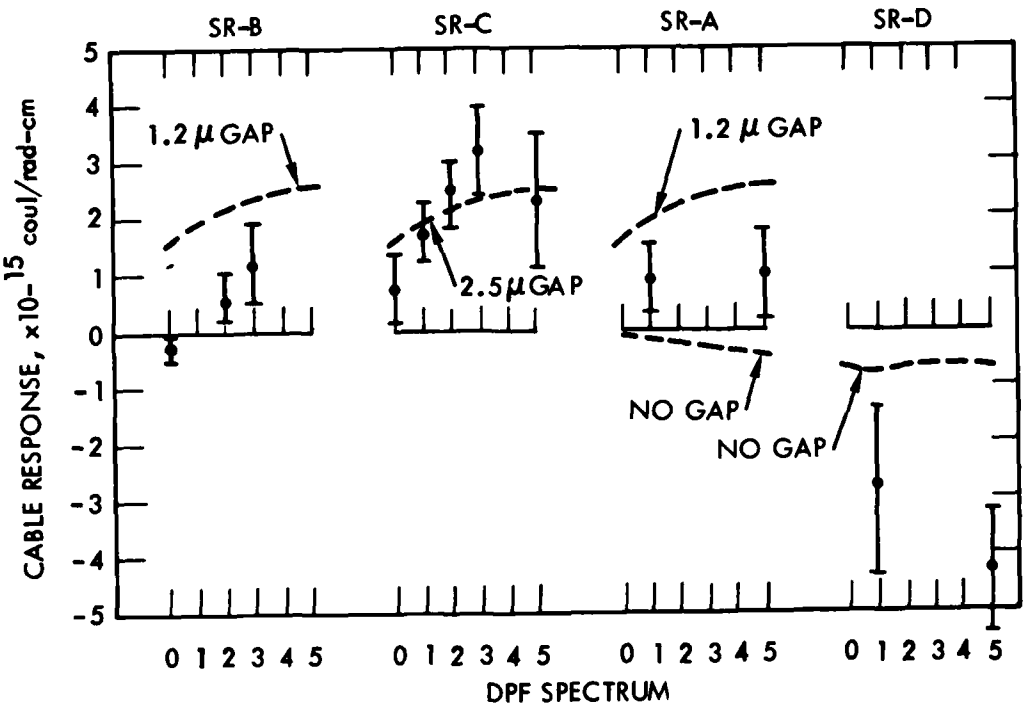

Figure 4.5-2. MCCABE model predictions for aluminum semi-rigid cables for the DPF spectra

pressure inside the cable itself was not measured, thus leaving the question open concerning outgassing difficulty.

The cross-over point, i.e., the air pressure where the "vacuum" response was sufficiently distorted, came at a few Torr, but the exact value was a function of the cable type and the size of its gap. The results are shown in Table 4.6-1 below.

Table 4.6-1. Cable response as a function of air pressure

	air pressure (Torr)						
Cable	$<10^{-5}$	1.5×10^{-3}	1.15×10^{-1}	0.56	1.3	2	3.8
BR-H (braided coax)	VAC	VAC	VAC	VAC	VAC	VAC	Air
SR-I (0.86" OD semi-rigid)	VAC	VAC	VAC	VAC	VAC	VAC	Air
BR-O (hollow semi-rigid)	VAC	VAC	VAC	Air	Air	Air	Air

The hollow semi-rigid cable has the largest gap between shield and insulation, and therefore can develop a larger potential in vacuum at the insulation interface compared to the other cables. The net result may be that the secondary conduction current in air may get a better opportunity to act at lower pressures than the other cables. In any case it is concluded that for the radiation testing of satellite qualified cables, a pressure of $<10^{-1}$ Torr is sufficient to guarantee a "vacuum-like" response.

4.7 Anomalous Cable Response

First shot anomalies are defined as occurring when the first shot peak response of a cable is substantially larger than the Nth shot, or equilibrium shot. This question was examined in some detail in an earlier report [9] and the conclusions at that time were that 1) such anomalies were seen only in semi-rigid cables, and 2) that they could be minimized if the samples were kept straight. It was hypothesized that outgassing in the bent samples might have something to do with the anomalous response.

For the present experiments it should be noted that a considerably larger variety of semi-rigid cables are being tested. It is of particular interest to see whether first shot anomalies might result in the aluminum/aluminum cables. The results are as follows: no anomalies were observed in any cables except the 0.086" OD copper/Teflon/silver-plated copper cable. This was the same type of cable that was giving the anomalous response in earlier investigations.[9] Four separate straight, virgin, 25 cm lengths of this cable were exposed, two to spectrum SPI-S, two to spectrum SPI-H. Only one of the samples (in the spectrum SPI-S configuration) showed a first shot anomaly;

the first shot response was about a factor of four above equilibrium (Figure 4.7-1). We are not completely certain of this factor, however, since the first shot response was only partially on-scale. The other identical sample that was sharing the cassette with this cable did not experience this anomalous behavior, but it is interesting to note that the equilibrium response of the former was a factor of eight lower than the cable which had an anomalous response. This is very disconcerting since one cannot, in all honesty, quote an equilibrium response for this cable to better than an order of magnitude.

In the samples tested in the harder spectrum, no anomalies were observed. After taking a few shots and observed no anomalies we then pumped down over the weekend, and we started shooting again; no noticeable change in signal was observed.

Finally we remark that an 0.086" OD cable sample was part of our air shot testing, described in sect. 4.6. The effect of the air pressure was to reduce the cable response, and make the signal bipolar, indicating the presence of a shunt air conductivity. Nothing like that is observed in these semi-rigid anomalies: the signal follows the pulse, but it reduces its amplitude from shot-to-shot. This casts doubt on the idea that it is air itself which is responsible for the anomalies.

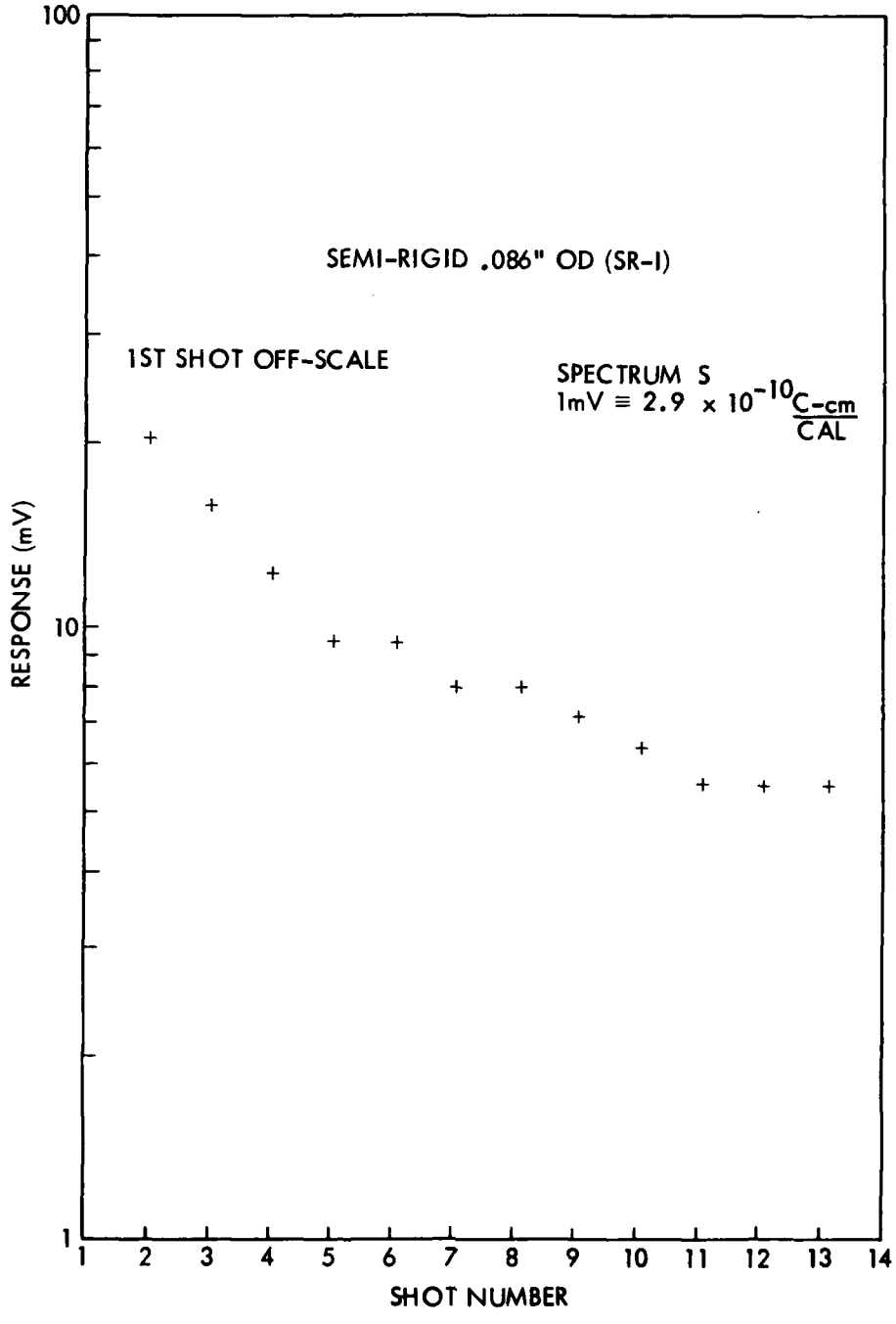

Figure 4.7-1. Anomalous response of 0.086" OD semi-rigid coax (SR-I)

5.0 CONCLUSIONS

An attempt has been made to pull together a quantitative comparison of SGEMP hardening approaches for cables in Table 5.1-1. However, there are other considerations in selecting cables for satellites then merely SGEMP response which is just one of the ingredients of the tradeoff matrix. Some of the disadvantages of the various hardening approaches are as follows:

Hardening Approach	Disadvantage
Increasing braid size	weight
Filling in gaps in braid cables	difficulty in practice
Using semi-rigid cable	lack of flexibility
Use solid dielectric (SiO_2)	cables must be hermetically sealed
Use aluminum semi-rigid	difficulty in making and maintaining connections

One possibility that seems most promising and has yet to be optimized is the use of conductive plastic coatings on the conductors. Of the samples tested only the shield-insulation interface has been treated. One could imagine treating the center wire(s) as well. In addition, reducing the resistivity of the conductive plastic by an order of magnitude seems possible, based on our discussions with Raychem. The main operational advantage is that it maintains the braided cable's flexibility.

We believe that the MCCABE model of x-ray response of cables is verified to about a factor of two for braided cables. For semi-rigid cables the model works less well, and we feel that this has more to do with uncertainties in assigning the gaps than in the model itself. In any case the relative response of cables which the MCCABE code predicted as a function of the various parameters, such as shield thickness, gap size, materials, etc. has been verified by the experimental results.

Table 5.1-1. Comparison of Hardening Approaches

Baseline	Hardening Approach	Response Reduction (DB)
Single braid	Double braid	0-12
Braid	Conductive plastic	6-16
Braid	Copper semi-rigid	4-12
Braid	Fill in gaps	12
Braid bundle	Braid coax	20
Semi-rigid, Teflon	Semi-rigid, Kel-F	4
Semi-rigid, Teflon	Semi-rigid, SiO_2	20
Semi-rigid, copper	Semi-rigid, aluminum	20

REFERENCES

1) V. van Lint, "Radiation-Induced Currents in Coaxial Cables," IEEE Trans. Nucl. Sci. NS-17, 210 (1970)

2) R. L. Fitzwilson, M, J. Bernstein and T. E. Alston, IEEE Trans. Nucl. Sci. NS-21, 276 (1974)

3) D. M. Clement, C. E. Wuller and E. Paul Chivington, "Multi-conductor Cable Response in X-ray Environments," IEEE Trans. Nucl. Sci. NS-23, 1946 (1976)

4) W. L. Chadsey, B. L. Beers, V. W. Pine, C. W. Wilson, "Radiation-Induced Signals in Cables," IEEE Trans. Nucl. Sci. NS-23, 1933 (1976)

5) D. M. Clement and C. E. Wuller, "Assessment of Cable Response Sensitivity to Cable and Source Parameter in Low Fluence X-ray Environments," DNA 4407 T, 8 April 1977

6) C. E. Wuller, L. C. Neilsen, D. M. Clement, "Definition of the Linear Region of X-ray Induced Cable Response," DNA 4405 T, 13 May 1977

7) D. M. Clement and C. E. Wuller, "MCCABE: A Code for Calculating X-ray Induced Currents in Shielded Cables," DNA , 28 February, 1978

8) F. Hai, P. A. Beemer, C. E. Wuller and D. M. Clement, "Measured and Predicted Radiation-Induced Currents in Semi-rigid Coaxial Cables," IEEE Trans. Nucl. Sci. NS-24, 2435 (1977)

9) D. M. Clement, L. C. Neilsen, T. J. Sheppard and C. E. Wuller, "Stored Charge Release in Cables in Low-Fluence X-ray Environments, "IEEE Trans. Nucl. Sci NS-24, 2422 (1977), and also DNA 4406 T, 8 April 1977

10) R. A. Lcwell, "X-ray Characterization of SPI-PULSE 6000," SPIRE TR-77-12, March, 1977

APPENDIX

PHOTOMICROGRAPHS OF CABLE SAMPLES

Most of the cable samples listed in Table 3.0-1 are shown in the following pages. Under each picture is the cable identifier corresponding to Table 3.0-1. Above each picture is the scale conversion factor which goes with the absolute scale at the bottom of each page.

1 DIVISION = 1/.40 cm

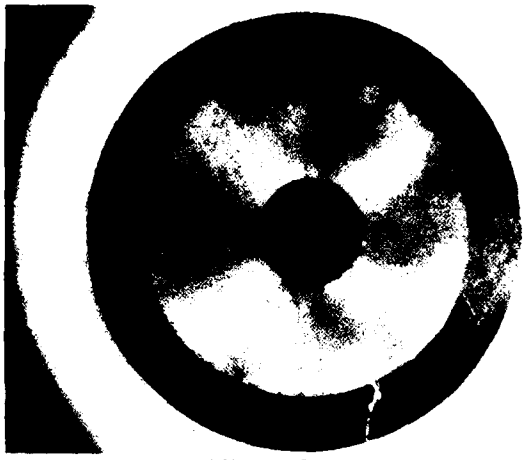

SR-A = ALUMINUM-TEFLON-ALUMINUM
.086" OD 50 Ω COAX

1 DIVISION = 1/35 m

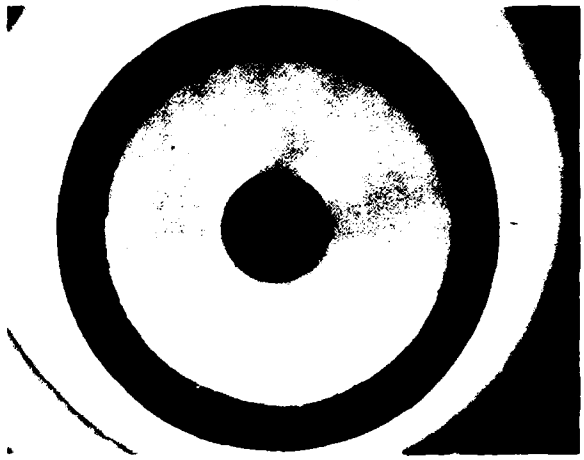

SR-B = ALUMINUM-TEFLON-ALUMINUM
.100" OD 50 Ω COAX

1 DIVISION = 1/35 cm

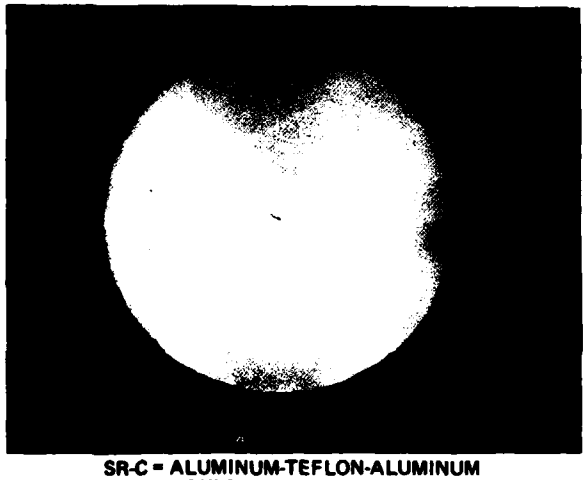

SR-C = ALUMINUM-TEFLON-ALUMINUM
.100" OD 100 Ω COAX

1 DIVISION = 1/22 cm

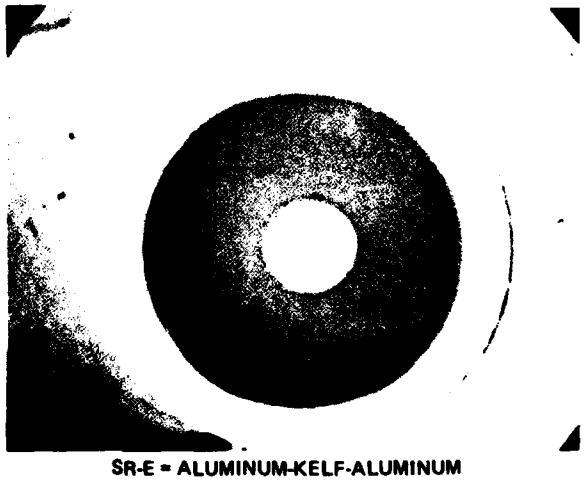

SR-E = ALUMINUM-KELF-ALUMINUM
.141" OD 50 Ω COAX

1 DIVISION = 1/30 cm

SR-D = ALUMINUM-TEFLON-ALUMINUM
.141" OD 50 Ω COAX

1 DIVISION = 1/28 cm

SR-F = ALUMINUM-HALAR-ALUMINUM
.141" OD 50 Ω COAX

SCALE

1 DIVISION

1 DIVISION = 1/22 cm

SR-G = ALUMINUM-TEFLON-COPPER
.141" OD 50 Ω COAX

1 DIVISION = 1/50 cm

SR-H = KOVAR-SILICON DIOXIDE-
COPPER .090" OD 50 Ω COAX

1 DIVISION = 1/35 cm

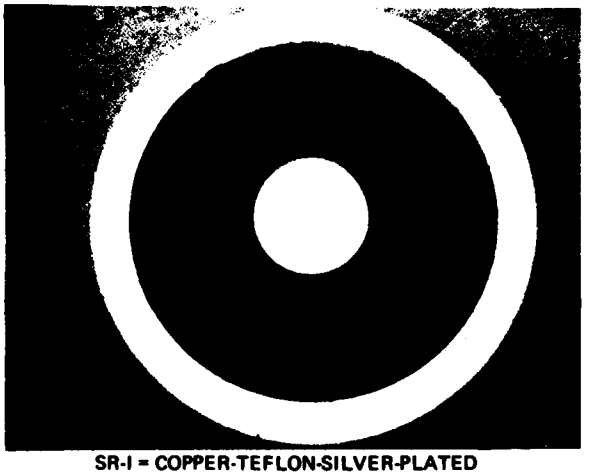

SR-I = COPPER-TEFLON-SILVER-PLATED
COPPER .086" OD 50 Ω COAX

1 DIVISION = 1/18 cm

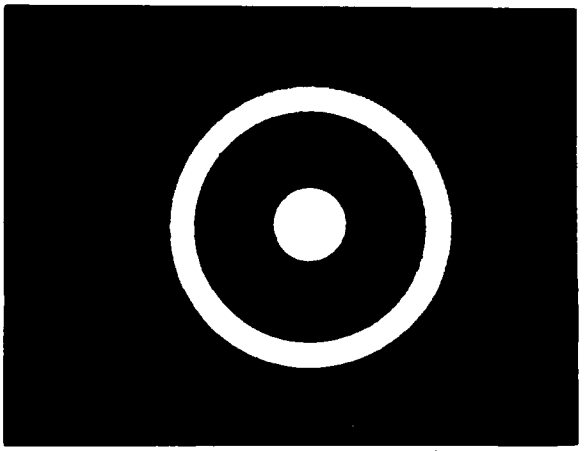

SR-J = COPPER-TEFLON-SILVER-PLATED
COPPER .141" OD 50 Ω COAX

1 DIVISION = 1/60 cm

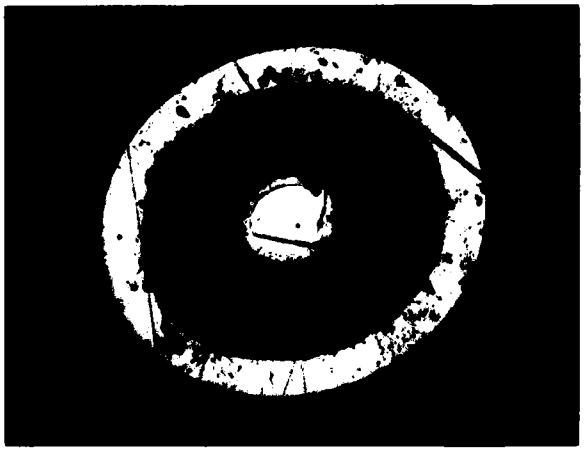

SR-K = COPPER-TEFLON-SILVER-PLATED
COPPER .046" OD 50 Ω COAX

1 DIVISION = 1/25 cm

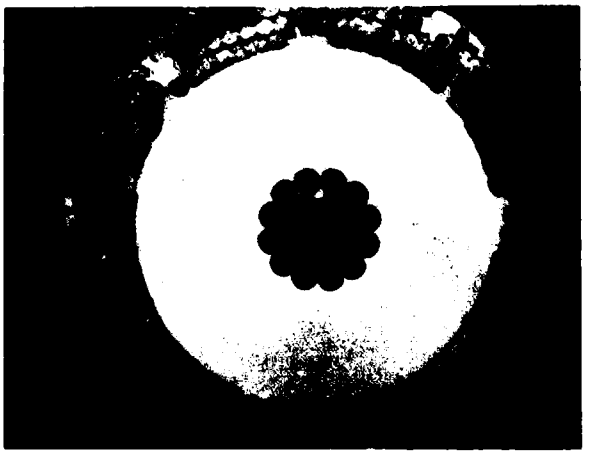

BR-A = DOUBLE ROUND
BRAID COAX

SCALE

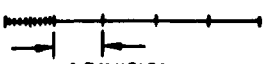

1 DIVISION

1 DIVISION = 1/20 cm

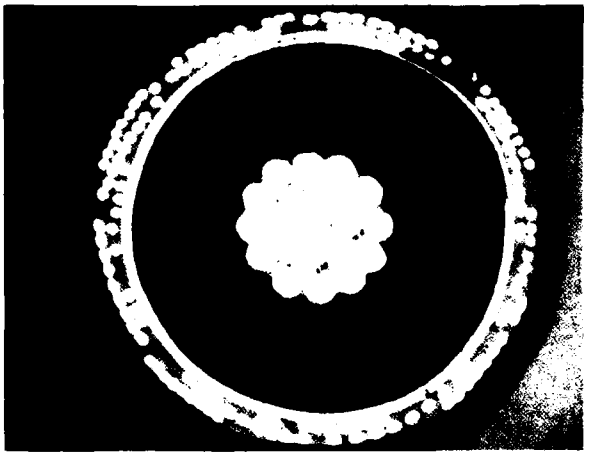

BR-B = OUTER ROUND BRAID + SOLID INNER SHIELD

1 DIVISION = 1/35 cm

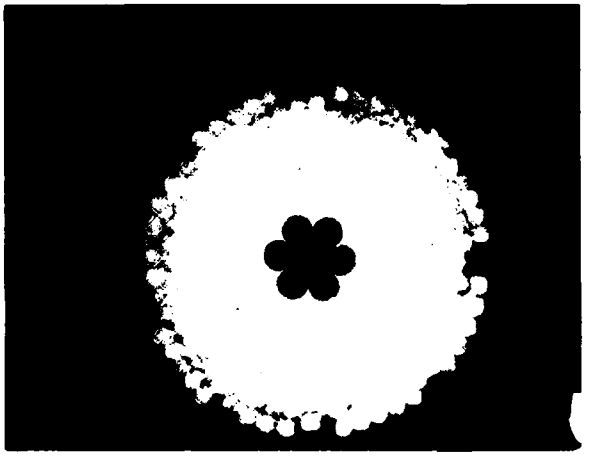

BR-C = RG316/U SINGLE ROUND BRAID

1 DIVISION = 1/35 cm

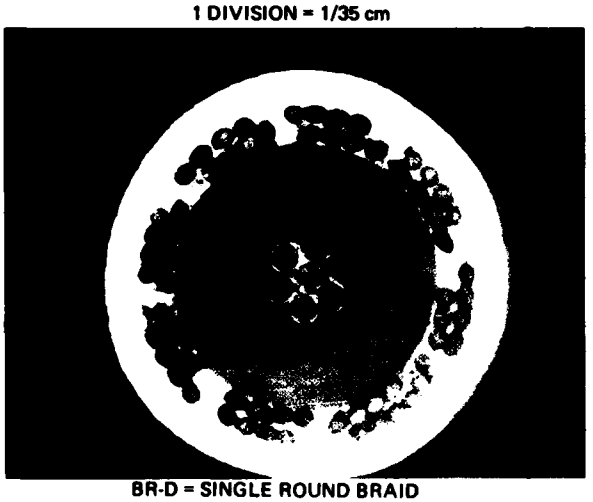

BR-D = SINGLE ROUND BRAID

1 DIVISION = 1/25 cm

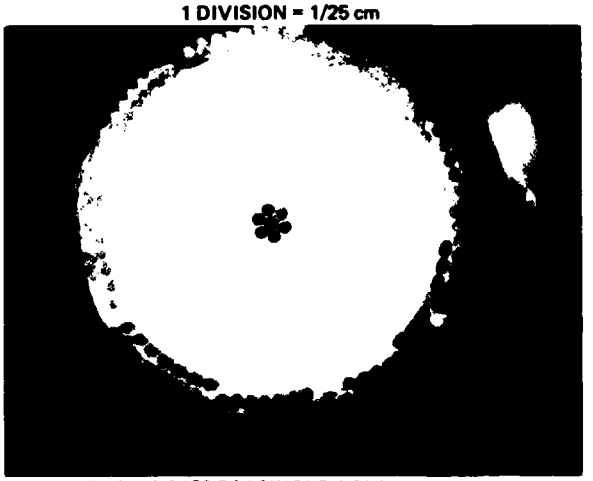

BR-E = RG180 B/U SINGLE ROUND BRAID

1 DIVISION = 1/65 cm

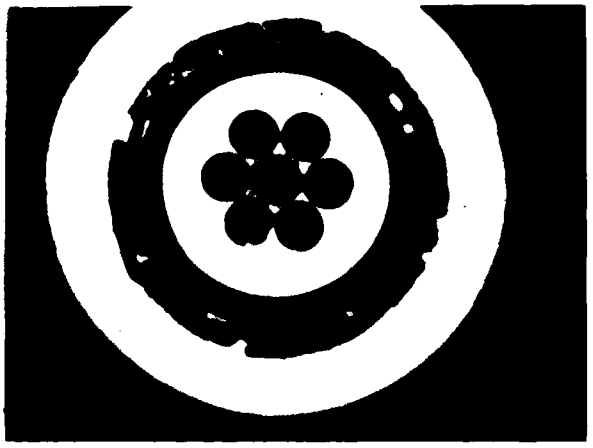

BR-F = SINGLE FLAT BRAID

1 DIVISION = 1/55 cm

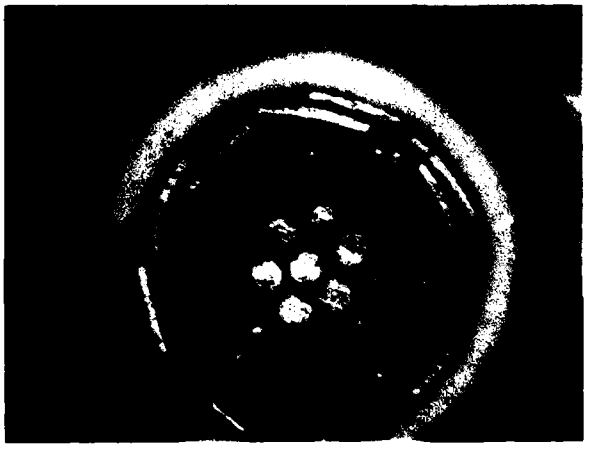

BR-G = SINGLE FLAT BRAID FOAMED DIELECTRIC

SCALE

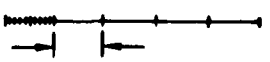

1 DIVISION

1 DIVISION = 1/55 cm

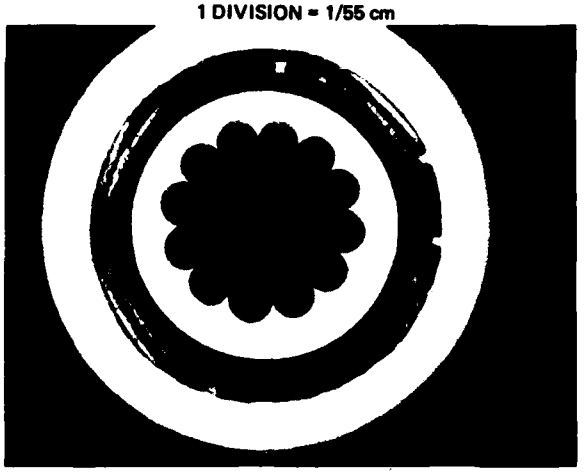

BR-H = SINGLE FLAT BRAID COAX

1 DIVISION = 1/23 cm

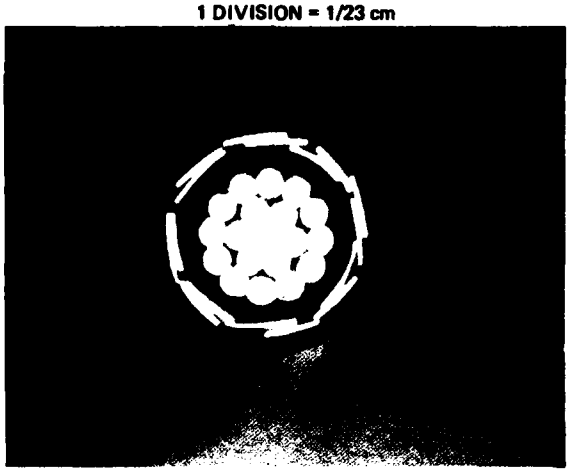

BR-I = SINGLE FLAT BRAID COAX

1 DIVISION = 1/30 cm

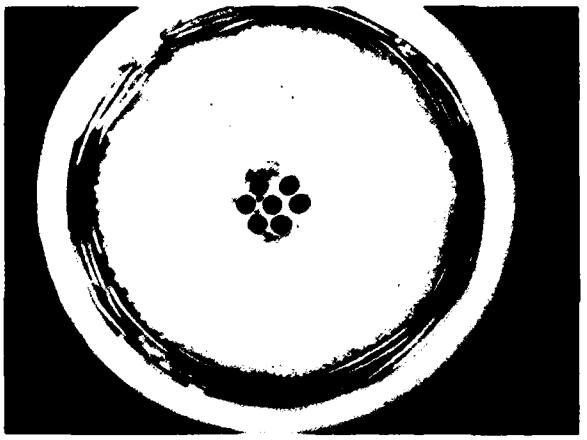

BR-J = DOUBLE FLAT BRAID COAX

1 DIVISION = 1/18 cm

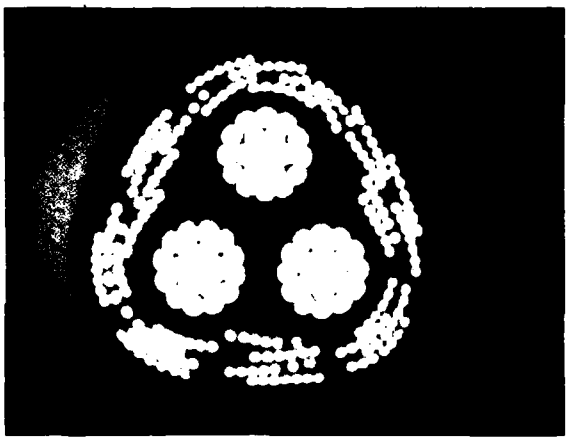

BR-K = DOUBLE ROUND BRAID 3-WIRE

1 DIVISION = 1/27 cm

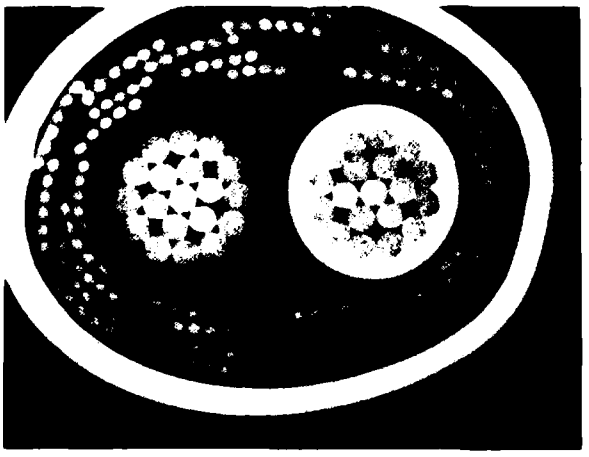

BR-L = DOUBLE ROUND BRAID 2-WIRE

1 DIVISION = 1/30 cm

BR-M = SINGLE FLAT BRAID 3 WIRE

SCALE

1 DIVISION

1 DIVISION = 1/40 cm

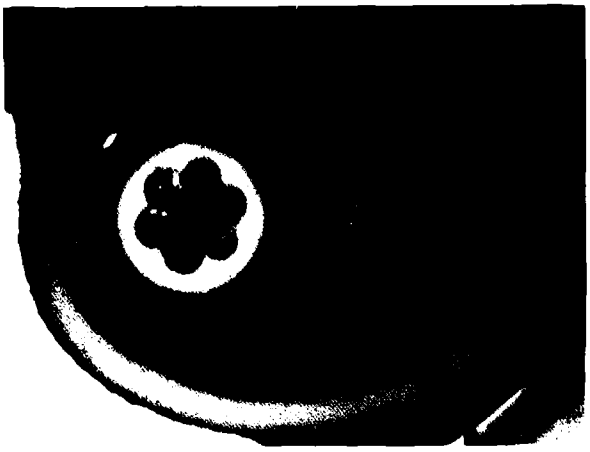

BR-N - SINGLE FLAT BRAID 2 WIRE

1 DIVISION = 1/6 cm

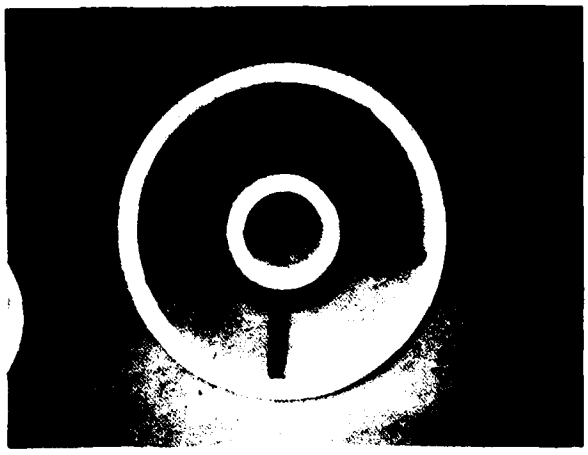

BR-O = HOLLOW SEMI-RIGID (SPLINE) COAX

1 DIVISION = 1/30 cm

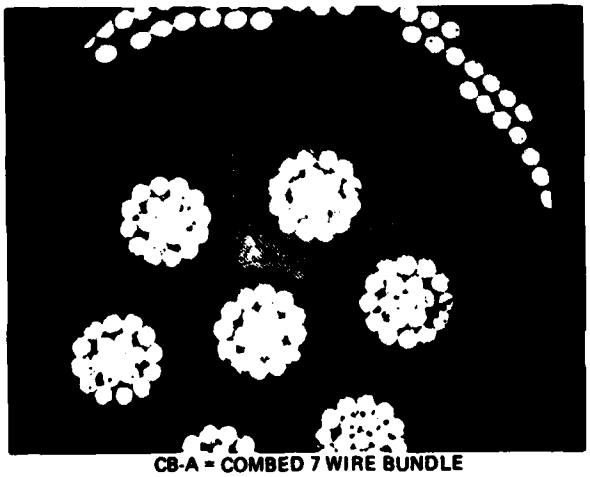

CB-A = COMBED 7 WIRE BUNDLE WITH SHIELD LINER

1 DIVISION = 1/30 cm

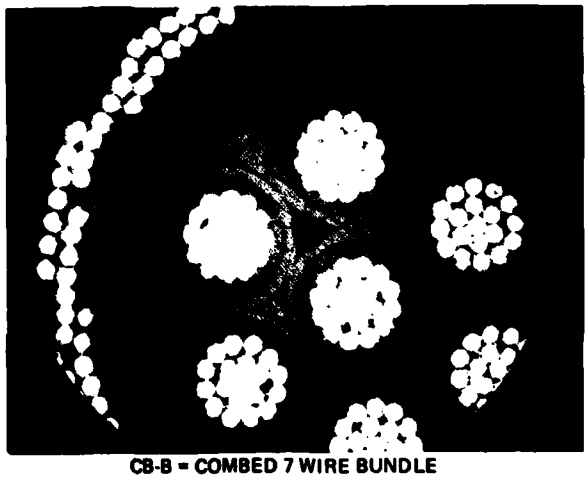

CB-B = COMBED 7 WIRE BUNDLE WITHOUT LINER

1 DIVISION = 1/10 cm

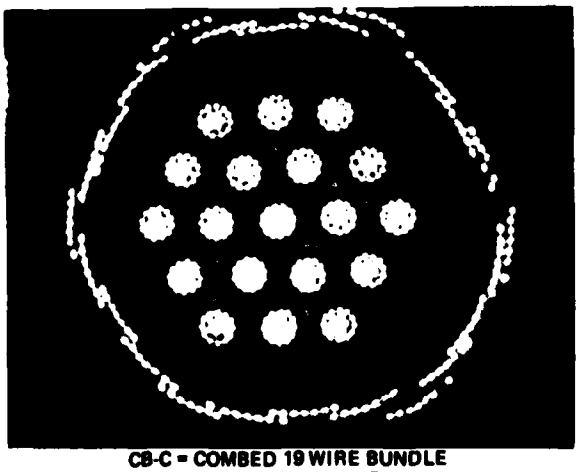

CB-C = COMBED 19 WIRE BUNDLE WITH SHIELD LINER

1 DIVISION = 1/40 cm

CB-D = 8 WIRE SILVER-EPOXY SHIELDED RIBBON CABLE

SCALE

1 DIVISION

1 DIVISION = 1/25 cm

SP-A = LOW RESISTIVITY TREATED

1 DIVISION = 1/20 cm

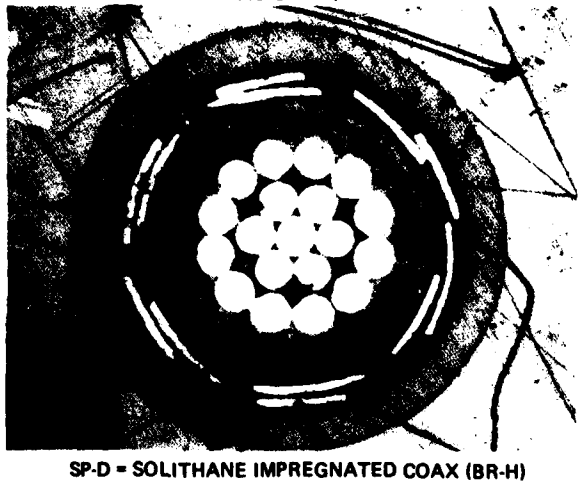

SP-D = SOLITHANE IMPREGNATED COAX (BR-H)

1 DIVISION = 1/30 cm

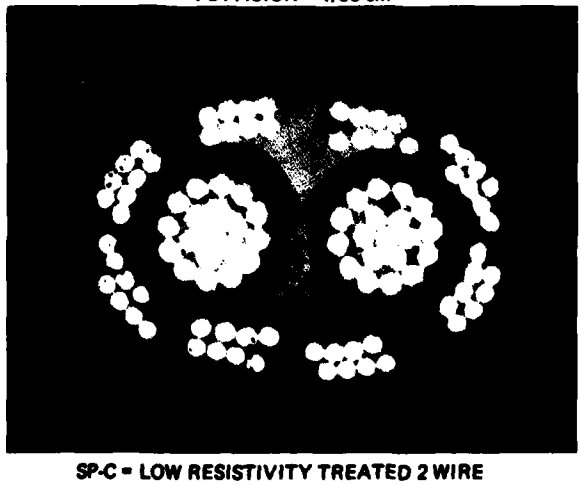

SP-C = LOW RESISTIVITY TREATED 2 WIRE

SCALE

1 DIVISION

DISTRIBUTION LIST

DEPARTMENT OF DEFENSE

Armed Forces Staff College
ATTN: Reference & Technical Svs Branch

Assistant Secretary of Defense
International Security Affairs
ATTN: Policy Plans & NSC Affairs

Assistant Secretary of Defense
Comm, Cmd, Cont & Intell
ATTN: Dir Survl & Warning Sys, W. Henderson

Assistant Secretary of Defense
Program Analysis & Evaluation
ATTN: Special Weapons & Support Systems Div
ATTN: Strategic Programs

Assistant to the Secretary of Defense
Atomic Energy
ATTN: Executive Assistant

Defense Advanced Rsch Proj Agency
ATTN: Director
ATTN: TIO
ATTN: Dir (Strat Tech Off)

Federal Emergency Management Agency
ATTN: Hazard Eval & Vul Red Div, G. Sisson

Defense Technical Information Center
12 cy ATTN: DD

Defense Intelligence Agency
ATTN: DT-1, M. Fletcher
ATTN: DT-1B, E. Decker
ATTN: DB-4C, E. O'Farrell
ATTN: DT-J, Vorona

Defense Nuclear Agency
24 cy ATTN: TITL
ATTN: Director

Field Command
Defense Nuclear Agency
ATTN: FCPR

Field Command
Defense Nuclear Agency
Livermore Division
ATTN: FCPRL

Joint Chiefs of Staff
ATTN: J-3, E. Burkhalter
ATTN: J-5, R. Lawson
ATTN: SAGA/SFD
ATTN: Director, Joint Staff

Joint Strat Tgt Planning Staff
ATTN: JLES, J. Enney
ATTN: JV, F. McMullen

Secretary of Defense Representative
Mutual & Balanced Force Reduction
DOD Mbfr Task Force
ATTN: R. Clarke

DEPARTMENT OF DEFENSE (Continued)

National Defense University
ATTN: Classified Library

National Security Agency
ATTN: Dir, B. Inman
ATTN: D-9, J. Amato

Net Assessment
Office of the Secretary of Defense
ATTN: A. Marshall

Secretary of Defense
ATTN: Special Assistant

Undersecretary of Defense for Rsch & Engrg
ATTN: Strategic & Space Systems (OS)

DEPARTMENT OF THE ARMY

Deputy Chief of Staff for Ops & Plans
Department of the Army
ATTN: DAMO-ZA, E. Meyer

Harry Diamond Laboratories
Department of the Army
ATTN: DELHD-N-P
ATTN: DELHD-N-TD, W. Carter

U.S. Army Materiel Dev & Readiness Cmd
ATTN: Commander

U.S. Army Nuclear & Chemical Agency
ATTN: Library

U.S. Army War College
ATTN: Library

DEPARTMENT OF THE NAVY

Naval Material Command
ATTN: R. Wertheim

Naval Surface Weapons Center
ATTN: Code X211

Naval War College
ATTN: Code E-11

Nuclear Weapons Plans Policy & Reg Br
Plans Policy & Operations, OCNO
Department of the Navy
ATTN: NSP-10

Office of Chief of Naval Operations
Department of the Navy
ATTN: OP 02
ATTN: OP 090
ATTN: OP 05
ATTN: OP 03
ATTN: OP 09, R. Long
ATTN: OP 009

Strategic Submarine Div OPNAV
Department of the Navy
ATTN: OP-21

DEPARTMENT OF THE AIR FORCE

Aerospace Defense Command
Department of the Air Force
ATTN: Commander

Air Force Institute of Technology
Air University
ATTN: Library

Air Force Office of Scientific Research
ATTN: NA, B. Wolfson

Air Force Systems Command
ATTN: CC, A. Slay
ATTN: DL

Air Force Weapons Laboratory
Air Force Systems Command
ATTN: SUL
ATTN: CC, W. Lehman

Air University Library
Department of the Air Force
ATTN: AUL-LSE-70-250

Assistant Chief of Staff
Intelligence
Department of the Air Force
ATTN: INA

Assistant Chief of Staff
Studies & Analyses
Department of the Air Force
ATTN: AF/SA, J. Welch, Jr.

Deputy Chief of Staff
Operations Plans and Readiness
Department of the Air Force
ATTN: AFXOO
ATTN: AFXO
ATTN: AFXOX

Deputy Chief of Staff
Research, Development & Acq
Department of the Air Force
ATTN: AFRDQ
ATTN: AFRD

Foreign Technology Division
Air Force Systems Command
ATTN: NIIS, Library
ATTN: SDBS, J. Pumphrey

Space & Missiles Systems Organization
Air Force Systems Command
ATTN: CC
ATTN: RS, L. Norris

Space & Missiles Systems Organization
Air Force Systems Command
ATTN: MN, J. Hepfer

DEPARTMENT OF THE AIR FORCE (Continued)

Strategic Air Command
Department of the Air Force
ATTN: XPFS, L. Leavitt
ATTN: DCS/Ops Plans
ATTN: DCS/Plans

DEPARTMENT OF ENERGY

Department of Energy
ATTN: ET
ATTN: OMA, D. Hoover
ATTN: ER-1, J. Deutch

DEPARTMENT OF ENERGY CONTRACTORS

Lawrence Livermore National Laboratory
ATTN: L-38, H. Reynolds
ATTN: L-203, L. Germain
ATTN: L-001, R. Batzel

Sandia National Laboratories
Livermore Laboratory
ATTN: T. Cook

Sandia National Laboratories
ATTN: Director
ATTN: R. Peurifoy
ATTN: Org 5000

OTHER GOVERNMENT

Central Intelligence Agency
ATTN: OSR Registry

Federal Preparedness Agency
General Services Administration
ATTN: S. Schmidt

U.S. Arms Control & Disarmament Agcy
ATTN: J. Young

DEPARTMENT OF DEFENSE CONTRACTORS

Aerospace Corp.
ATTN: W. Mann

AVCO Research & Systems Group
ATTN: J. Stevens

BDM Corp.
ATTN: J. Braddock

Boeing Co.
ATTN: V. Jones

Brookhaven National Laboratory
Technical Support Org for Safeguards
ATTN: J. Indusi

R. E. Dougherty
ATTN: R. Dougherty

G. A. Kent
ATTN: G. Kent

DEPARTMENT OF DEFENSE CONTRACTORS (Continued)

General Electric Co.
Reentry & Environmental Systems Div.
ATTN: C. Raver

General Electric Co.
Aerospace Grp Strat Planning & Prgms Ops
ATTN: R. Minckler
ATTN: D. Rodgers

General Electric Company—TEMPO
ATTN: DASIAC

General Research Corp.
ATTN: Technical Information Office

Henry S. Rowen
ATTN: H. Rowen

Hercules, Inc.
ATTN: Library

Institute for Defense Analyses
ATTN: J. Bengston

JAYCOR
ATTN: J. Young

Kaman Sciences Corp.
ATTN: A. Bridges
ATTN: D. Osborn

Lockheed Missiles and Space Co., Inc.
ATTN: Document Control

M.I.T. Lincoln Lab
ATTN: L. Loughlin

DEPARTMENT OF DEFENSE CONTRACTORS (Continued)

University of Miami
ATTN: F. Kohler

Northrop Corp.
ATTN: D. Hicks

Pacific-Sierra Research Corp.
ATTN: F. Thomas

Pan Heuristics
Science Applications, Inc.
ATTN: A. Wohlstetter

R & D Associates
ATTN: C. MacDonald

Rockwell International Corp.
ATTN: J. Howe

Santa Fe Corp.
ATTN: D. Paolucci

Science Applications, Inc.
ATTN: J. Martin

System Planning Corp.
ATTN: J. Douglas

Systems, Science & Software, Inc.
ATTN: Document Control

TRW Defense & Space Sys Group
ATTN: D. Scally
ATTN: D. Clement
ATTN: R. Lowell

TRW Defense & Space Sys Group
ATTN: J. Gorman